

DIELECTROPHORESIS OF SOLIDS IN LIQUIDS OF DIFFER-
FERING DIELECTRIC CONSTANT AND CONDUCTIVITY

By

CYPRIAN M. FEELEY

Bachelor of Arts

University of Dublin

Ireland

1964

Submitted to the faculty of the Graduate College
of the Oklahoma State University
in partial fulfillment of the requirements
for the degree of
MASTER OF SCIENCE
August, 1969

NOV 5 1969

DIELECTROPHORESIS OF SOLIDS IN LIQUIDS OF DIFFER-
ENT DIELECTRIC CONSTANT AND CONDUCTIVITY

Thesis Approved:

Herbert A. Pohl

Thesis Adviser

Thomas S. Kinter

D. D. Burham

Dean of the Graduate College

729936

ACKNOWLEDGEMENTS

Many people in the Physics Department have been of assistance in this research and in the production of this thesis. I am indebted firstly to my Advisor, Dr. H. A. Pohl, who presented me with this research problem. His continual encouragement was invaluable and his support of my attendance at scientific meetings helped greatly. I also owe thanks to: Dr. E. E. Kohnke who supplied crystals of rutile and cassiterite, to J. S. Crane for his most helpful discussions on the problem, to D. Mickish for his assistance with the computer program, and finally to the Research Foundation who funded this investigation. In addition, I would like to thank Mrs. Janet Sallee for typing this thesis so competently.

TABLE OF CONTENTS

Chapter	Page
I. INTRODUCTION.	1
II. THEORY.	4
III. APPARATUS AND EXPERIMENTAL PROCEDURE.	9
Test Cell and Electrodes	9
Electrodes and the Electric Field.	11
The Liquid Medium.	11
Measurements of Resistivity.	13
Particles.	15
Method	15
IV. RESULTS	18
V. SUMMARY AND CONCLUSIONS	41
Brief Summary of the Work.	41
Conclusions.	41
The Enhancement of Bulk Liquid Polarization by Ions.	44
The Enhancement of Polarization of Solids by Ionic Double Layer.	44
BIBLIOGRAPHY.	46
APPENDIX. COMPUTING PROGRAM.	48

LIST OF TABLES

Table	Page
I. Dielectric Constants of the Water/Dioxane Mixture.	12
II. Values of Dielectric Constants and Specific Resistivities Used	16

LIST OF FIGURES

Figure	Page
1. Platinum Electrode Cell.	10
2. Resistance Probe Construction.	14
3. Deflection Versus Voltage Squared for Silicon Dioxide at 2.55 MHz	19
4. Slope Versus Dielectric Constant of Liquid for Silicon . .	20
5. Slope Versus Dielectric Constant of Liquid for Silicon Dioxide.	21
6. Slope Versus Dielectric Constant of Liquid for Tin	22
7. Slope Versus Dielectric Constant of Liquid for Stannic Oxide.	23
8. Slope Versus Dielectric Constant of Liquid for Lead Haf- nate	24
9. Slope Versus Dielectric Constant of Liquid for Rutile. . .	25
10. Slope Versus Dielectric Constant of Liquid for Silicon . .	27
11. Slope Versus Dielectric Constant of Liquid for Silicon Dioxide.	28
12. Slope Versus Dielectric Constant of Liquid for Tin	29
13. Slope Versus Dielectric Constant of Liquid for Stannic Oxide.	30
14. Slope Versus Dielectric Constant of Liquid for Lead Haf- nate	31
15. Slope Versus Dielectric Constant of Liquid for Rutile. . .	32
16. Calculated Slope Z_{calc} Versus Observed Slope Z_{obs} for Sil- icon	34
17. Calculated Slope Z_{calc} Versus Observed Slope Z_{obs} for Sil- icon Dioxide	35

LIST OF FIGURES (Continued)

Figure	Page
18. Calculated Slope Z_{calc} Versus Observed Slope Z_{obs} for Tin.	36
19. Calculated Slope Z_{calc} Versus Observed Slope Z_{obs} for Stannic Oxide.	37
20. Calculated Slope Z_{calc} Versus Observed Slope Z_{obs} for Lead Hafnate.	38
21. Calculated Slope Z_{calc} Versus Observed Slope Z_{obs} for Rutile	39
22. Schematic Structure, and Energy Levels Before and After Sorption of Surface Negative Ions.	43

CHAPTER I

INTRODUCTION

The seventeenth century saw the first scientific work in the field of dielectrophoresis, and there were individual observations of the phenomenon in the eighteenth century^{1,2,3}. With the increased use of electricity in technology in the first half of the twentieth century various effects unaccountable in terms of electrophoretic forces were observed. This led to work in the field of liquid dielectrics.

These early experiments and discussions in the field of liquid dielectrics involved treating the dielectrics as perfect dielectrics^{4,5}. The experiments were limited to, the observation of the phenomenon, or its use to determine the dielectric constants of liquids. Several experimenters, while studying electrophoresis, unknowingly observed dielectrophoresis. Hatschek and Thorne⁶, experimenting on the effect of an electric field on nickel sols in toluene, noticed that these small particles migrated under the influence of the electric field, but unexpectedly did not reverse their direction of motion upon reversal of the field. Soyenoff⁷ attributed the coalescence of dust particles in high electric fields to dielectric polarization, and was the first to note that any suspended body of higher conductivity or dielectric constant than the suspending medium moves towards the region of highest field strength. However, it was not until 1951 that dielectrophoresis was named and defined by H. A. Pohl⁸.

Work since 1951 on dielectrophoresis has been for the most part concerned only with the behavior of insulating solids and liquids⁹ with the view of effecting the purification of polymers and fuels, and the determination of molecular weights. There is good agreement between theory and experiment when these substances are theoretically treated as ideal dielectrics¹⁰. However, Pohl and Hawk in dielectrophoresis experiments of lossy materials in water observed anomolous results inexplicable using simple theory¹¹. The simple field theory did not take account of the fact that the dielectrics were not perfect insulators.

Dielectrophoresis is the motion of matter induced by the polarising action of a non-uniform electric field. This phenomenon differs from that of electrophoresis in that in electrophoresis translational motion of a charged particle occurs in a uniform electric field.

When a non-uniform electric field is applied to a system consisting of a suspended particle in a liquid dielectric both substances become polarized. If the particle is more polar than the liquid it will experience a net force into the region of highest field intensity. But if the particle is less polar than the liquid the particle will move to the locus of lowest field intensity. Interestingly this holds for both A.C. and D.C. non-uniform electric fields. The equation of force for a spherical particle in a weakly divergent field can be shown to be¹².

$$\vec{F} = 2\pi a^3 \epsilon_0 \frac{K_1 (K_2 - K_1)}{K_2 + 2K_1} \vec{\nabla} |\vec{E}|^2 \quad \text{I-1}$$

where \vec{F} = force, a = radius of sphere, K_1, K_2 = static dielectric constants of the liquid and the solid respectively, ϵ_0 = permittivity

of free space, and \vec{E} = external field. $|\vec{E}|$ is the r.m.s. value of the electric field strength. If the particle is charged, then in A.C. dielectrophoresis the net electrophoretic force over a cycle is zero. The predictions made using this equation agree with experiment when using poorly conducting materials¹⁰.

For lossy dielectrics in a time varying field, that is for those whose dielectric loss components are comparable to the real component, it was found that the previous force equation (I-1) is invalid¹¹. Here the absolute static dielectric constants must be replaced by absolute complex dielectric constants, i.e., replace ϵ_1 by $\epsilon_1 = \epsilon_1 - \frac{i}{\omega\rho}$ where ρ = specific resistivity ohms - meter, and ω = angular frequency, and making the K_1 factor the complex conjugate. In this case the force on a sphere can be shown¹³ to be

$$\vec{F} = \frac{3}{2} V_1 \operatorname{Re} \left\{ \epsilon_1^* \left(\frac{\epsilon_2 - \epsilon_1}{\epsilon_2 + 2\epsilon_1} \right) \right\} \vec{V} |\mathbf{E}|^2 \quad (\text{I-2})$$

where * denotes complex conjugate, and V_1 is the volume of the sphere.

The present work investigated the dielectrophoretic response of six particles differing in electrical properties, and in liquids of varying dielectric constants. This response was measured as a function of frequency to determine frequency dependence. The effect of varying the resistivity of the liquid medium on the dielectrophoretic response at high frequency was also observed. The experimental results thus obtained were compared with those predicted by the above equation.

CHAPTER II

THEORY

The dielectrophoretic force equation for non-ideal dielectrics is obtained by considering the variation of the electrical energy in the electrical field upon the introduction of a dielectric body. The energy in the field for a linear dielectric is given by

$$w = \frac{1}{2} \int_v \vec{E} \cdot \vec{D} \, dv, \quad \text{II-1}$$

the integral being taken over a volume v . The energy change due to the introduced body is

$$\Delta w = \frac{1}{2} \int (\vec{E}_2 \vec{D}_2 - \vec{E}_1 \vec{D}_1) \, dv, \quad \text{II-2}$$

the subscripts indicating the values before and after its introduction. In the A.C. field the electric and displacement vectors are not assumed to be in phase and are represented by complex quantities $\vec{E} = \vec{E} \exp(i\omega\tau)$ and $\vec{D} = \vec{D} \exp(i\omega\tau)$. The complex dielectric constant is introduced $\epsilon = \epsilon' - i\epsilon''$, the imaginary part being due to the loss of current in the dielectric $\epsilon'' = G/\omega$, where G equals conductivity and ω equals angular frequency. The real part is the dielectric constant normally used to characterize the storage of charge in a capacitance. Both parts are normally frequency dependent.

The electric field and displacement are physical quantities and the real parts are taken in the calculation of the time average of the

energy change

$$\Delta \bar{w} = \frac{1}{2} \int_V \overline{\text{Re}(\vec{E}_2) \text{Re}(\vec{D}_2)} - \overline{\text{Re}(\vec{E}_1) \text{Re}(\vec{D}_1)} dv, \quad \text{II-3}$$

the bar indicating the time average values. However, since both \vec{E} and \vec{D} are simple harmonic functions of time, and as shown by Stratton¹⁴.

$$\overline{\text{Re}(\vec{E}) \text{Re}(\vec{D})} = \frac{1}{2} \text{Re}(\vec{E}^* \vec{D}), \quad \text{II-4}$$

where the asterisk denotes the complex conjugate, then

$$\Delta \bar{w} = \frac{1}{4} \text{Re} \int_V (\vec{E}_2^* \vec{D}_2 - \vec{E}_1^* \vec{D}_1) dv. \quad \text{II-5}$$

The integral can be simplified by means of an identity given by G. Schwarz²⁰, using the relation

$$\text{Re}(\vec{E}_2^* \vec{D}_2 - \vec{E}_1^* \vec{D}_1) = \text{Re} \left\{ \left(\vec{E}_2 - \frac{\epsilon_1}{\epsilon_1^*} \vec{E}_1 \right)^* (\vec{D}_2 - \vec{D}_1) + \left(\vec{E}_2 \vec{D}_1^* - \frac{\epsilon_1^*}{\epsilon_1} \vec{E}_1^* \vec{D}_2 \right) \right\} \quad \text{II-6}$$

where ϵ_1 equals the dielectric constant of the liquid medium. The term on the right hand side is zero outside the volume of the body V, since $\vec{D}_2 = \epsilon_1 \vec{E}_2$ and the remaining part of this theory shows that the mean energy is an integral function of this term. The first term may be written

$$\left(\vec{E}_2 + \frac{\epsilon_1}{\epsilon_1^*} \vec{E}_1 \right)^* (\vec{D}_2 - \vec{D}_1) = - (\vec{D}_2 - \vec{D}_1) \text{grad} \left(\psi_2 + \frac{\epsilon_1}{\epsilon_1^*} \psi_1 \right)^* = - (\vec{D}_2 - \vec{D}_1) \text{grad} \phi^* \quad \text{II-7}$$

\vec{E}_2 and \vec{E}_1 being the negative gradients of the complex potentials ψ_2 and ψ_1 and $\phi = \psi_2 + \frac{\epsilon_1}{\epsilon_1^*} \psi_1$. This first part of (II-7) can be further re-

duced by means of the identity

$$- (\bar{D}_2 - \bar{D}_1) \text{grad } \phi^* = - \text{div} \{ \phi^* (\bar{D}_2 - \bar{D}_1) \} + \phi^* \text{div} (\bar{D}_2 - \bar{D}_1), \quad \text{II-8}$$

which gives

$$- (\bar{D}_2 - \bar{D}_1) \text{grad } \phi^* = - \text{div} \{ \phi^* (\bar{D}_2 - \bar{D}_1) \}, \quad \text{II-9}$$

since $\text{div } \bar{D} = \rho$ leads to $\text{div} (\bar{D}_2 - \bar{D}_1) = 0$ since the charge distribution is fixed. Using (II-9) and Gauss's theorem gives

$$- \int (\bar{D}_2 - \bar{D}_1) \text{grad } \phi^* \, dv = - \lim_{S_0 \rightarrow \infty} \int \phi^* (\bar{D}_2 - \bar{D}_1) \, d\bar{f} + \sum_j \int_{S_j} \phi^* (\bar{D}_2 - \bar{D}_1) \, d\bar{f}, \quad \text{II-10}$$

The first closed surface integral taken over the surface S_0 , goes to zero as the surface increases to an infinite size, for ϕ^* will be nearly proportional to r^{-1} , \bar{D} to r^{-2} and the area to r^2 . The integral is then nearly proportional to r^{-1} .

The total change in the mean energy (II-6) is

$$\begin{aligned} \bar{\Delta w} &= \frac{1}{4} \text{Re} \int_V (\bar{E}_2^* \bar{D}_2 - \bar{E}_1^* \bar{D}_1) \, dv, \\ &= \frac{1}{4} \text{Re} \sum_j \int_{S_j} \phi (\bar{D}_2 - \bar{D}_1) \, d\bar{f} + \frac{1}{4} \text{Re} \int_V (\bar{E}_2 \bar{D}_1^* - \frac{\epsilon_1^*}{\epsilon_1} \bar{E}_1^* \bar{D}_2) \, dv. \end{aligned} \quad \text{II-11}$$

In general $\int_S \bar{D} \, d\bar{f} = \text{charge}$ so the first term equals the time mean of the work done at the charged conductors present in the system. Subtracting it from $\bar{\Delta w}$ gives the mean energy of the introduced body.

This expression can be rewritten as

$$\Delta \bar{u} = \frac{1}{4} \operatorname{Re} \int_v \left\{ \epsilon_1^* \left(1 - \frac{\epsilon_2}{\epsilon_1} \right) \bar{E}_2 \bar{E}_1^* \right\} dv, \quad \text{II-13}$$

using the relations $\bar{D}_2 = \epsilon_2 \bar{E}_2$ and $\bar{D}_1 = \epsilon_1 \bar{E}_1$.

It is assumed that the field is weakly divergent to the extent that the field inside the introduced spherical dielectric body is homogeneous to a first approximation. The internal field is then

$$\bar{E}_2 = \frac{3\epsilon_1}{\epsilon_2 + 2\epsilon_1} \bar{E}_1. \quad \text{II-14}$$

Substituting this in (II - 14) gives

$$\Delta \bar{u} = \frac{3}{4} \operatorname{Re} \int_v \left[\frac{\epsilon_1 \epsilon_1^*}{\epsilon_2 + 2\epsilon_1} \left(1 - \frac{\epsilon_2}{\epsilon_1} \right) \bar{E}_1 \cdot \bar{E}_1^* \right] dv, \quad \text{II-15}$$

$$\text{but } E_1^* \cdot E = |E|^2, \quad \text{II-16}$$

therefore

$$\Delta \bar{u} = -\frac{3}{2.2} \operatorname{Re} \int_v \frac{\epsilon_1^* (\epsilon_2 - \epsilon_1)}{\epsilon_2 + 2\epsilon_1} |E|^2 dv, \quad \text{II-17}$$

$$= -\frac{3}{2} \operatorname{Re} \int_v \frac{\epsilon_1^* (\epsilon_2 - \epsilon_1)}{\epsilon_2 + 2\epsilon_1} E_o^2 dv, \quad \text{II-18}$$

where E_o the r.m.s. value of the field.

$$E_o = |E|/\sqrt{2}. \quad \text{II-19}$$

The force on the body is given by

$$\vec{F} = - \vec{\nabla} (\Delta \bar{u}), \quad \text{II-20}$$

$$= \frac{3}{2} V \operatorname{Re} \frac{\epsilon_1^* (\epsilon_2 - \epsilon_1)}{\epsilon_2 + 2\epsilon_1} \vec{\nabla} (E_o^2), \quad \text{II-21}$$

if ϵ not $\epsilon(x)$; and where V is the volume of the body, this free equation reduces to the well known expression for loss-free dielectrics

$$\bar{F} = \frac{3}{2} V \epsilon_1' \frac{(\epsilon_2' - \epsilon_1')}{\epsilon_2' + 2\epsilon_1'} \vec{\nabla} (E_o^2), \quad \text{II-22}$$

the dielectric constants ϵ' being real.

CHAPTER III

APPARATUS AND EXPERIMENTAL PROCEDURE

Test Cell and Electrodes

To observe the dielectrophoretic response of a particular particle a test cell was used in which the particle was suspended between two electrodes. This test cell was constructed of a Pyrex tube fitted with an optically flat glass window. The window was thin enough to allow observation of the particle by a 100X microscope, the eyepiece of which contained a graduated reticle.

The particle was suspended by a fine glass fiber (some 4.5 cm long) between the electrodes, the particle being attached to the fiber by means of a minute amount of an insoluble epoxy cement. The fiber itself was supported by wedging it in a hole drilled in a teflon spacer between the electrodes.

The electrode system was constructed of two parallel platinum wires of 1.02 mm diameter, separated by teflon spacers at a distance of 2.1 mm. They were supported by thin teflon arms from a large teflon support. The large support passed through a teflon plug inserted in the pyrex tube.

These electrodes were polished as far as possible with crocus cloth and chemically cleaned using a solution of ether and HCl.

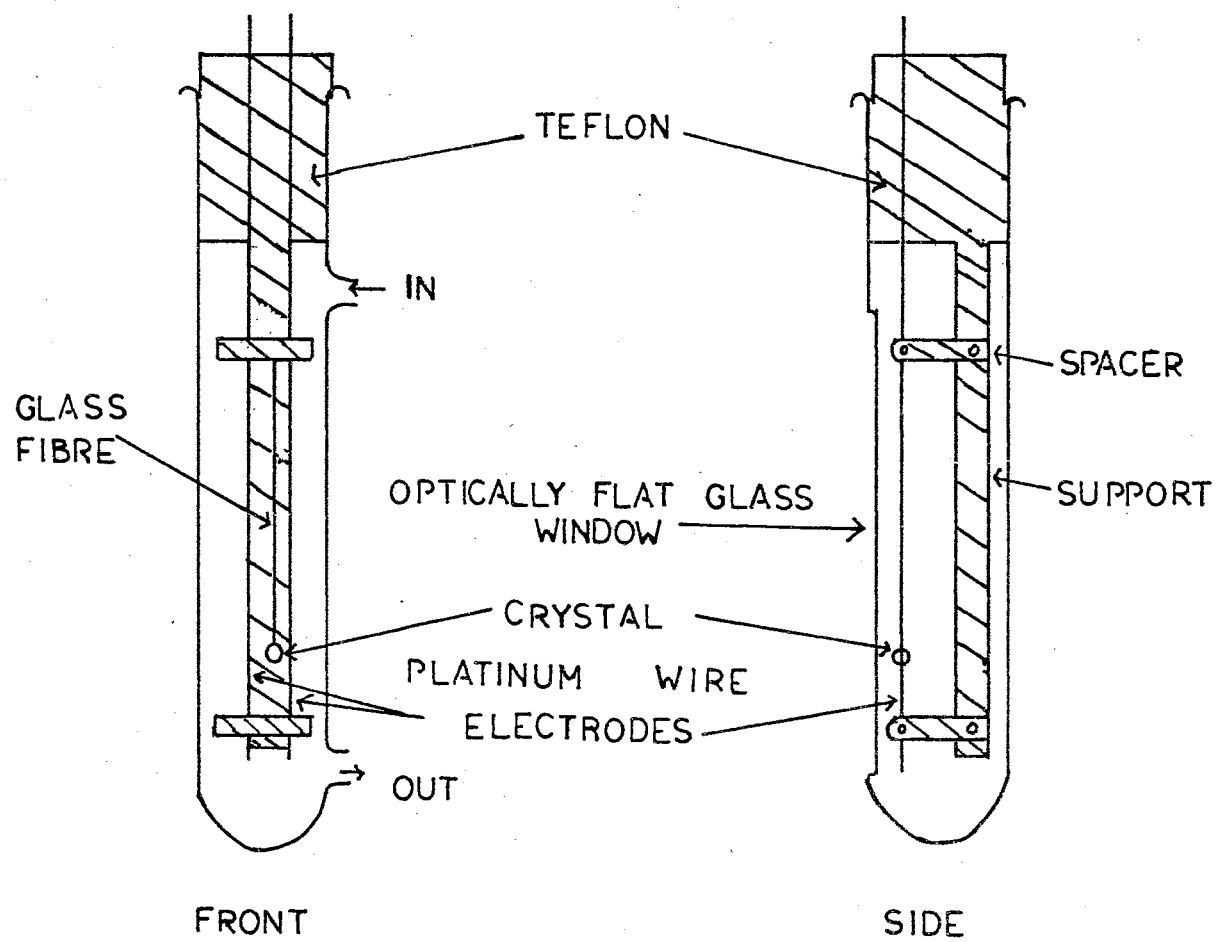


Figure 1. Platinum Electrode Cell

Electrodes and the Electric Field

Platinum electrodes were used as their electrode polarization is less than that of most other materials. The polarization due to the double layer of charge on the surface of the electrodes reduces the field strength for conducting liquids at low frequencies. This double layer has an electrical impedance inversely proportional to its capacitance and frequency. As a result the applied potential drops steeply over the double layer and the electric field in the liquid changes with frequency. Therefore, the dielectrophoretic response in lossy media is more properly measured at high frequencies.

The electric field was produced across the electrodes by applying the amplified voltage from an audio frequency (0.1 KHz - 10 KHz) generator: Hewlett Packard 200 CD. The audio amplifier used was a Heath A9. A separate high frequency 2.5 MHz voltage source capable of producing 200 volts r.m.s. was also used. The voltage across the electrodes was measured using a Hewlett Packard 410B radio frequency voltmeter (frequency response 20 Hz - 200 MHz).

The Liquid Medium

The dielectrophoretic response of particles was observed in mixtures of dioxane and water over a dielectric constant range of 2.2 to 79. Dioxane was chosen as it is readily miscible in water and by addition of water the dielectric constant of the mixture could therefore be easily increased. Mixtures were prepared having the dielectric constants 2.2, 3.5, 4.4, 5.8, 9.0, 12.0, 37, and 79. The proportions of water to dioxane were those given by Kraus and Fuoss, as shown in Table

TABLE I
DIELECTRIC CONSTANTS OF THE WATER/DIOXANE MIXTURE

Composition of Liquid		Dielectric Constant
$C_4H_3O_2$	H_2O	
100.0	0.0	2.20
95.99	4.01	3.5
93.63	6.37	4.4
90.50	9.50	5.8
85.05	14.95	9.0
79.77	20.23	12.0
47.0	53.0	37
0.0	100.0	78.6

The resistivity for a particular dielectric constant value of the liquid medium was altered by the addition of the salt tetra-iso-pentyl-ammonium nitrate (Eastman Kodak). This salt was chosen as it readily dissolves in dioxane and in water. The addition of the salt to water depresses the dielectric constant very little, and not importantly (for example, 10 M in water depressed it from 80 to 79.8¹⁶). At each dielectric constant of the liquid medium three different resistivities were used.

In the preparation of the mixtures, high resistivity ($10^5 \Omega$ meter) distilled water was used, this being obtained by passing distilled water through a mixed bed ion-exchanger.

Measurements of Resistivity

A resistance probe with bright platinum electrodes of approximate area $40 \text{ (mm}^2\text{)}$ and separated by a distance of 1 mm was used to measure the resistance of the liquid media. The rest of the probe supporting the electrodes was made of polyacetal-resin, with insulated platinum wires running through it to the electrodes. To obtain the cell constant for the probe it was calibrated against another probe, a Yellow Springs Instrument Company. Model 3400 conductivity cell with known cell constant.

Resistances up to $10^5 \Omega\text{-m}$ were easily measured by the alternating current method. The probe with a variable nulling capacitor ($10^{-7} \text{ F} - 10^{-10} \text{ F}$) formed one arm of a Wheatstone Bridge. The remainder of the Bridge consisted of a 1650 B General Radio Bridge, complete with a null detector.

The resistance could be measured over the frequency range 100 Hz -

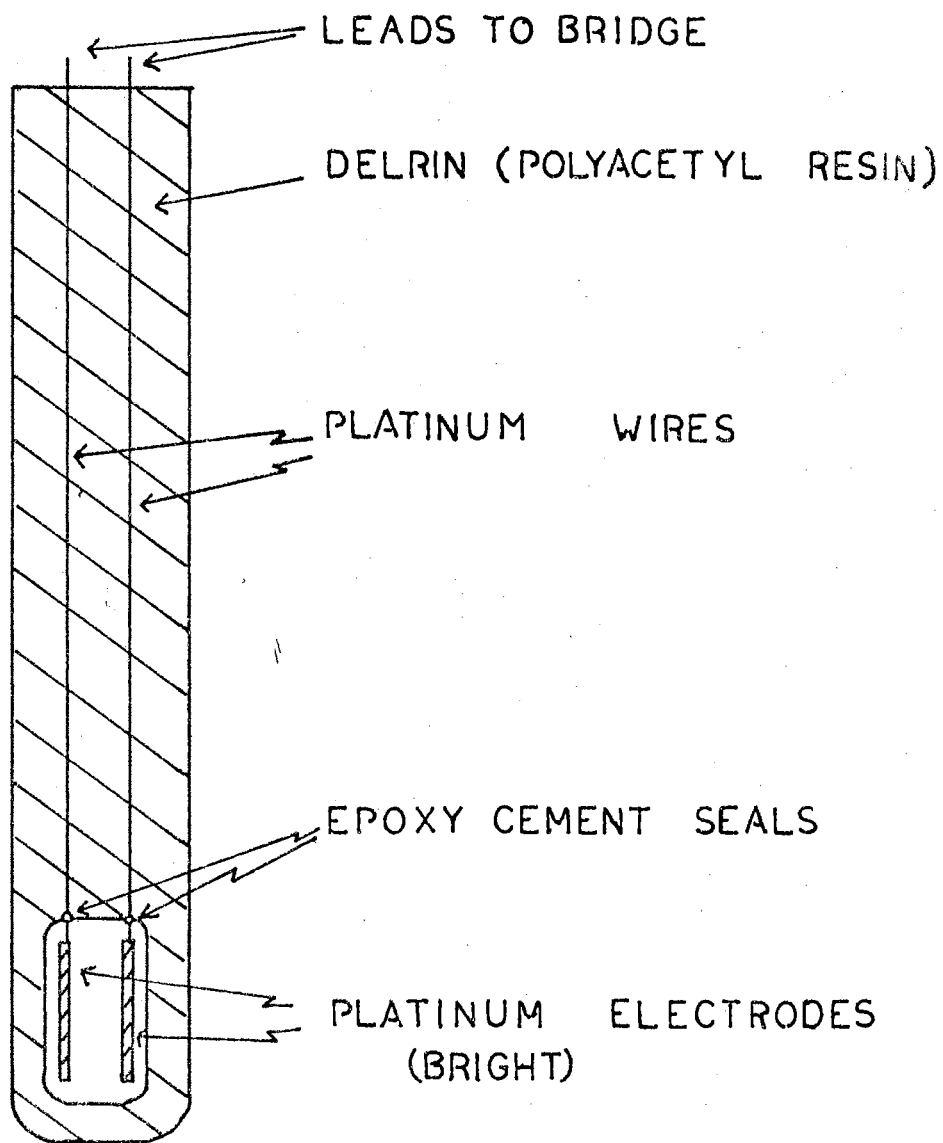


Figure 2. Resistance Probe Construction

20 KHz by applying the output from an audio frequency generator to the 1650 B Bridge. In the experiment the resistance of the liquid media was measured before and after its use in the dielectrophoresis cell.

Particles

Particles of six different materials were studied: silicon, silicon dioxide, tin, stannic oxide, rutile, and lead hafnate. These particles had no sharp edges and were roughly spherical in shape, having been polished by means of a small cylindrically shaped air centrifuge. The centrifuge wall was covered with a fine abrasive paper. The air entered through the cylinder wall of the centrifuge tangentially and the resulting rapid stirring motion caused the particles to hit against the cylinder wall.

The values of dielectric constant and resistivity for the particles are given in Table II. The silicon dioxide has a high D.C. resistivity. The A.C. resistivity is taken not to vary significantly over the frequency range used in this experiment. The variation of resistivity with frequency was measured for silicon and lead hafnate and was found to be insignificant.

The dielectric constants of lead hafnate and cassiterite were measured as a function of frequency by G. Baum and the variation for the purpose of this experiment was taken to be negligible ¹⁷.

Method

A particular particle was suspended in the test cell which was filled with a liquid medium of known dielectric constant, the liquid medium of lowest dielectric constant being used first so that the resis-

TABLE II

VALUES OF DIELECTRIC CONSTANTS AND SPECIFIC RESISTIVITIES USED

Material	Dielectric Constant	Frequency	Reference Source	Resistivity (ohm-meter)	Reference
silicon	11.9	13 GHz	A	5.0×10^2	E
silicon dioxide	3.78	1 MHz	B	10^{16}	C
tin	-----	-----	-	1.1×10^{-4}	F
stannic oxide	24	1 GHz	C	2.7×10^3	E
rutile			B	1.0×10^4	G
(∥ optic axis)	170	1 MHz	B		
(⊥ optic axis)	86	1 MHz	B		
lead hafnate	350	1 MHz	D	10^{16}	E

A - H. B. Briggs, Phys. Rev., 77, 287 (1950).

B - A. von Hippel, Dielectric Materials and Applications, pub. jointly by the Tech. Press of M.I.T. and John Wiley and Sons, Inc., New York (1954).

C - Handbook of Chemistry and Physics, pub. by Chemical Rubber Co., 37th ed.

D - Dr. E. E. Kohnke, Okla. State University, private communication.

E - Measured in our laboratory.

F - Lange Handbook.

G - D. C. Cronmeyer, Phys. Rev. 87, 896 (1951).

tivity of the media decreased with each successive run. At zero voltage # the particle was positioned at a fixed distance near one of the electrodes and this distance was maintained over the complete range of dielectrics of the liquid media. A run was started by filling the cell with the liquid medium of lowest dielectric constant. For a particular frequency the voltage necessary to cause different deflections was recorded and tables of deflection against voltage for each resistivity and frequency were recorded. The cell was then emptied slowly and the resistance of the medium measured. Before refilling for the next run with a medium of higher dielectric constant the cell was carefully rinsed with this next medium.

The Equation (II-10) indicates that the dielectrophoretic force varies as the r.m.s. voltage squared. Assuming Hooke's Law to hold for small displacements of the particle from zero field equilibrium position the deflection observed was taken to be directly proportional to the voltage squared. Graphs of deflection against voltage squared were plotted. From these the initial slopes at the origin were determined. The theoretical dielectrophoretic force (Z_{calc}) for unit applied voltage is seen from Equation (II-10) to be directly proportional to

$$\epsilon_1 \frac{(\epsilon_2 - \epsilon_1)}{\epsilon_2 + 2\epsilon_1}$$

The value of this slope for a particular set of resistivities and dielectric constants is computed using the program shown.

CHAPTER IV

RESULTS

To illustrate the dielectrophoretic response the data was plotted as graphs of deflection against voltage squared as shown, e.g., in Figure 3. At the origin the slope gave a measure of the force per unit voltage. This initial slope $Z_{obs.}$ was plotted against the dielectric constant of the liquid medium. The graphs for different conditions are in three sets exhibiting: firstly how the force on different particles behaves with frequency in liquids of differing dielectric constant, secondly, how the force on the particles changes when the salt tetra-iso-pentylammonium nitrate is added, and thirdly, how the experimentally determined initial slope correlates with that predicted by the theory Equation II-10).

Interestingly the results predicted by the ideal dielectric force Equation (II-22), in which the real dielectric constants are replaced by complex dielectric constants, agree with those deduced from the analytically rigorous force Equation (II-21), when they are compared utilizing the experimental values of dielectric constants and resistivities.

Furthermore, the computer print-out shows that the theoretical dielectrophoretic force is not sensitive to large changes in the resistivity of the particles (i.e., changes of the order 10^5 ohms-meter), but is sensitive to small changes in the resistivity of the liquid medium (i.e., of the order < 10 ohms-meter).

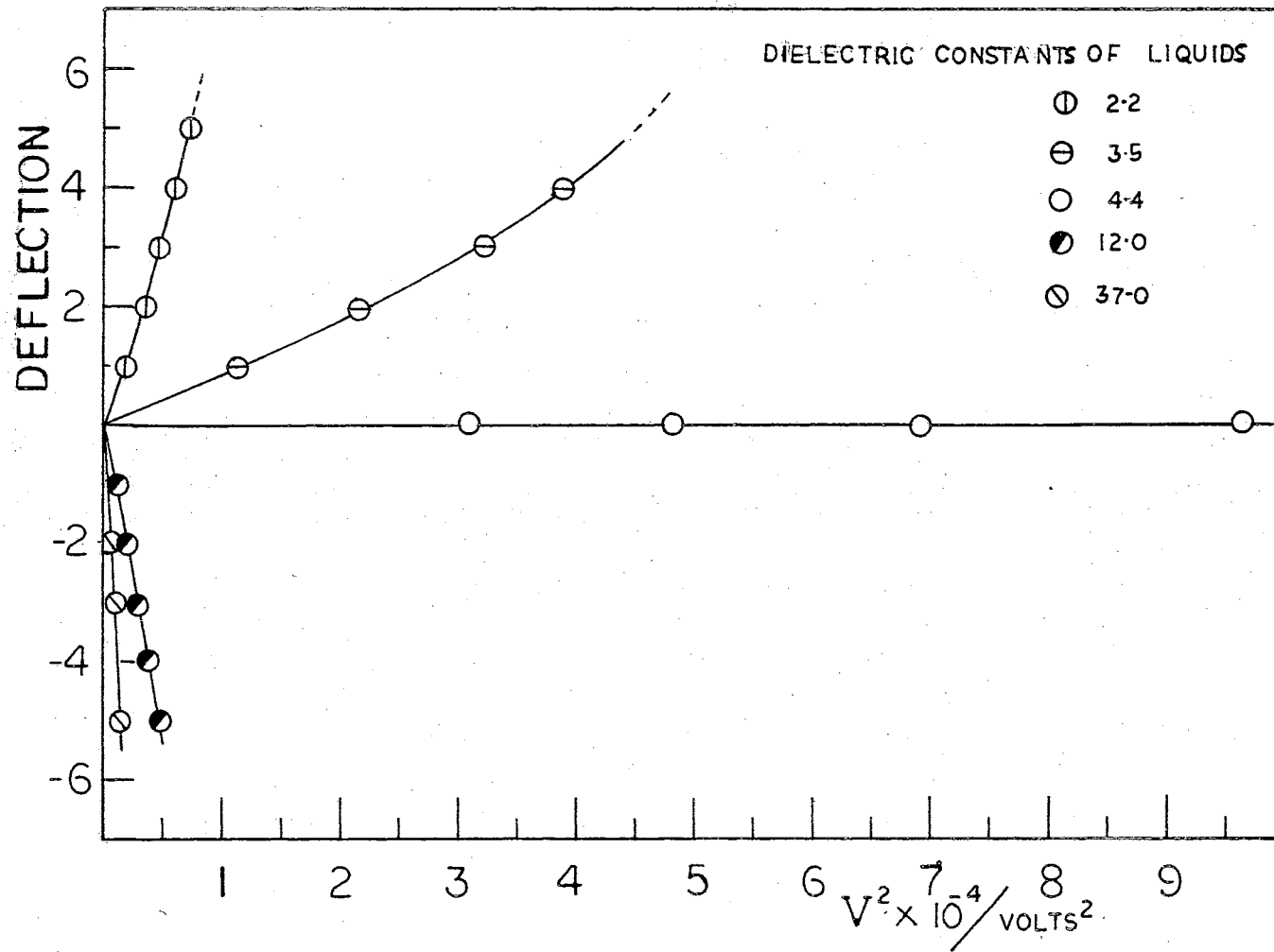


Figure 3. Deflection Versus Voltage Squared for Silicon Dioxide at 2.55 MHz

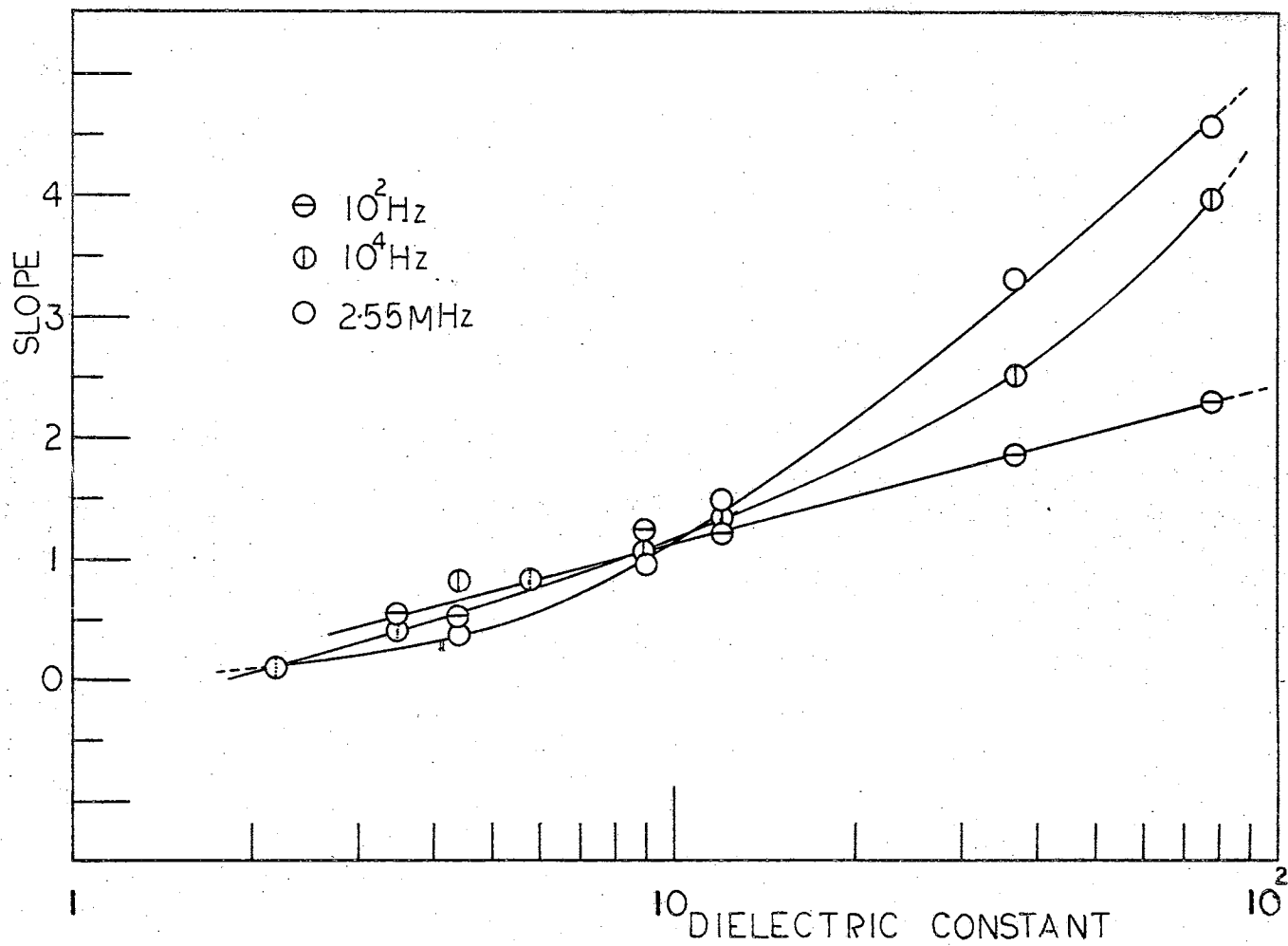


Figure 4. Slope Versus Dielectric Constant of Liquid for Silicon

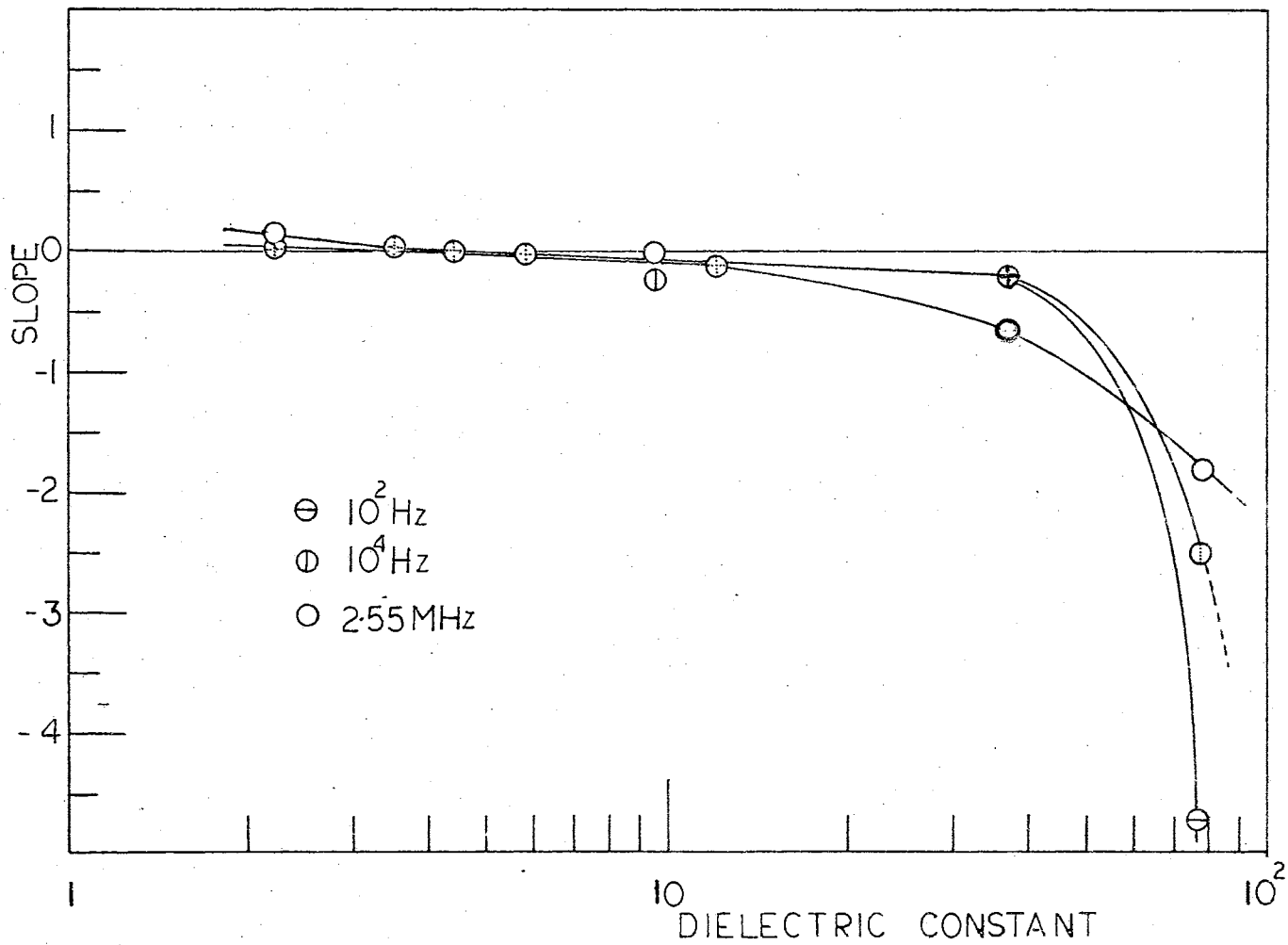


Figure 5. Slope Versus Dielectric Constant of Liquid for Silicon Dioxide

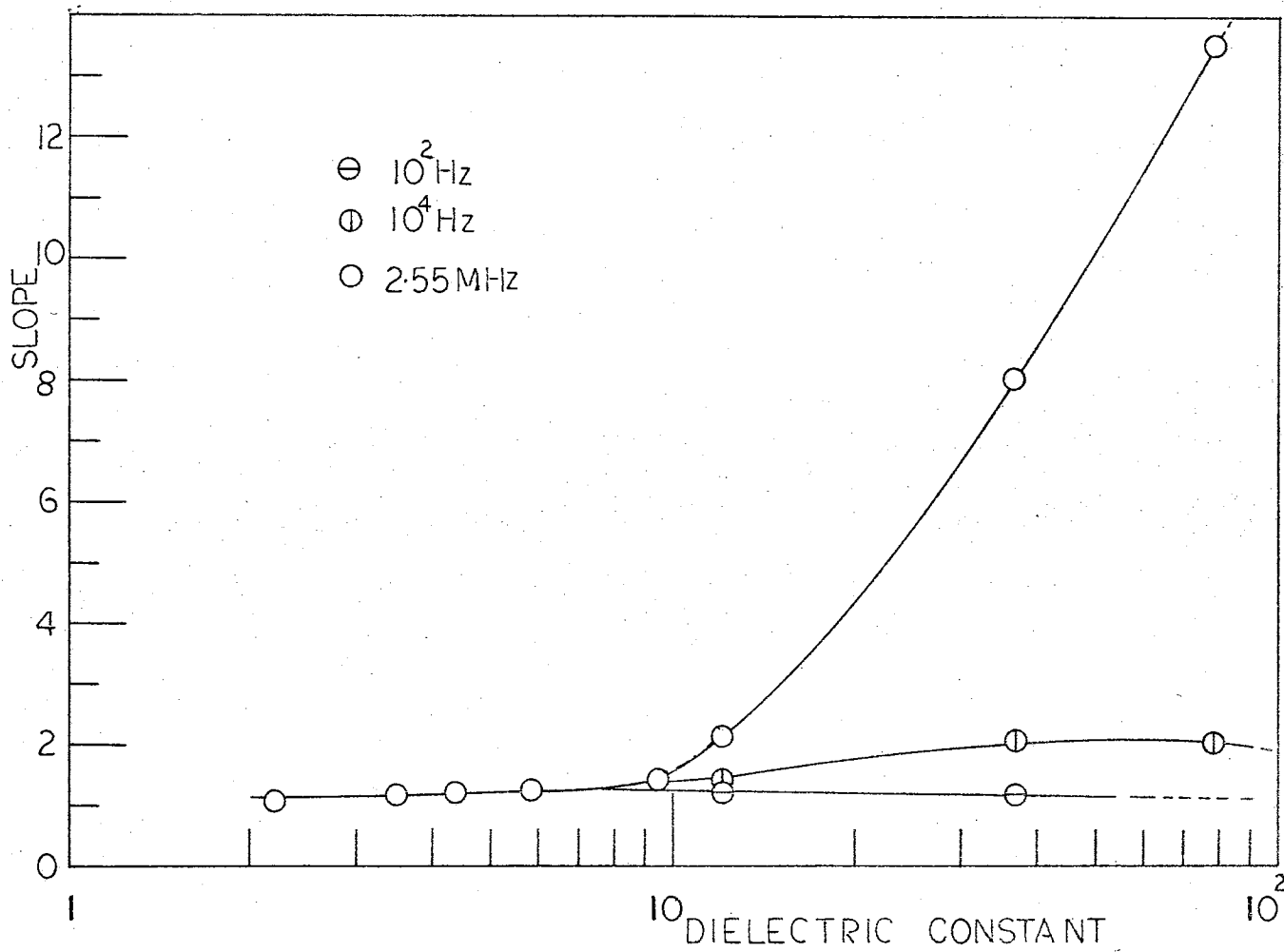


Figure 6. Slope Versus Dielectric Constant of Liquid for Tin

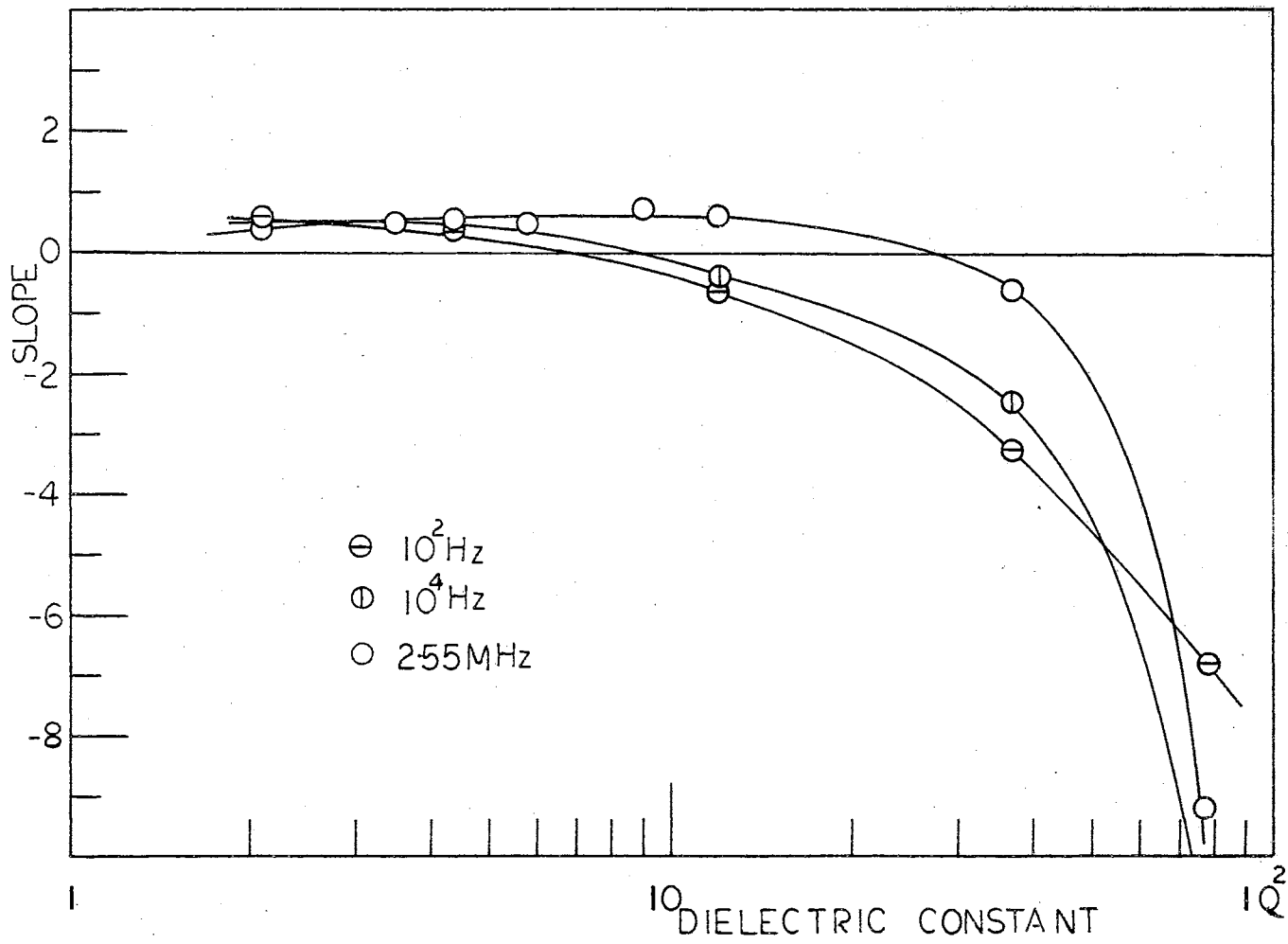


Figure 7. Slope Versus Dielectric Constant of Liquid for Stannic Oxide

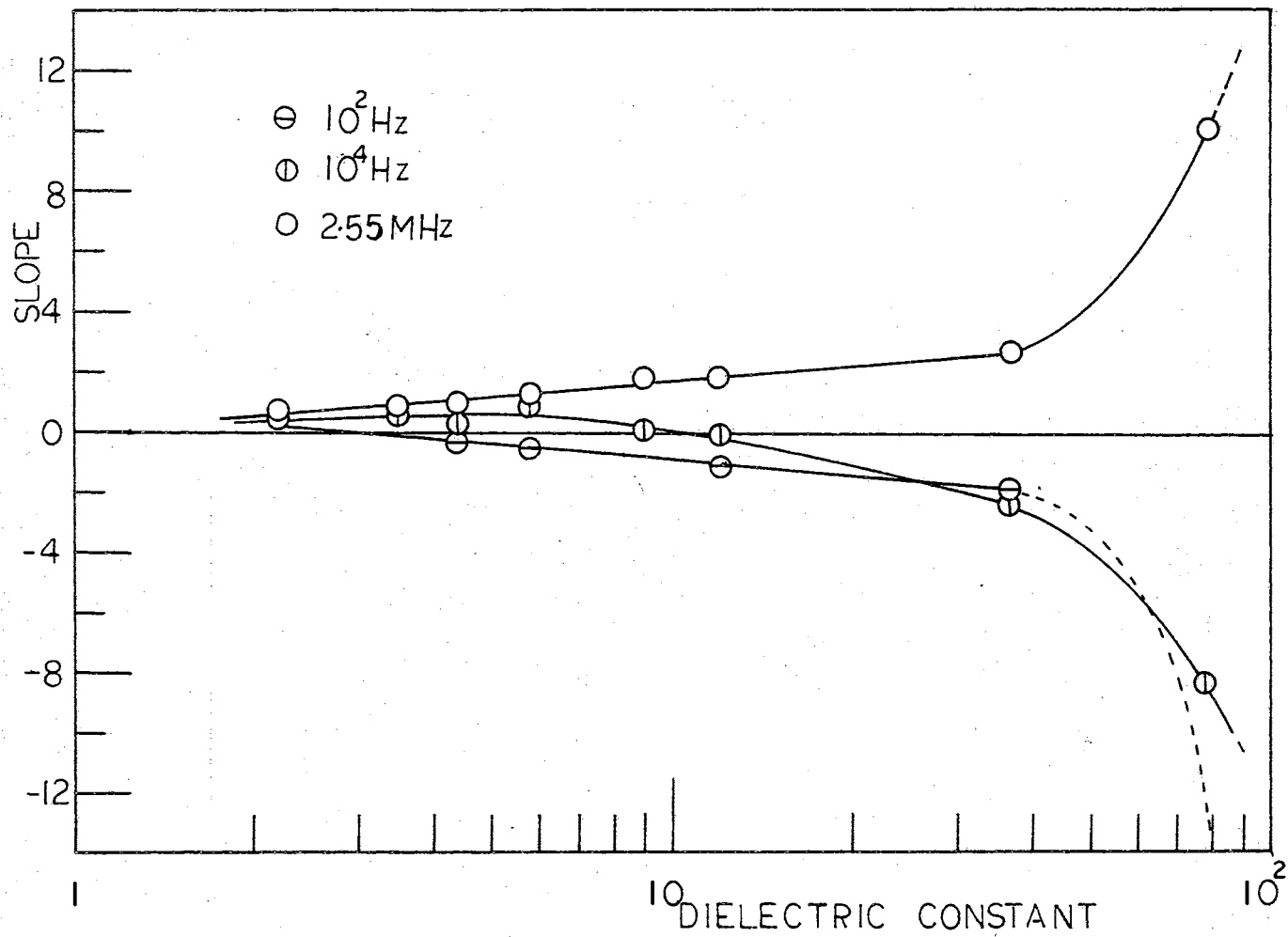


Figure 8. Slope Versus Dielectric Constant of Liquid for Lead Hafnate

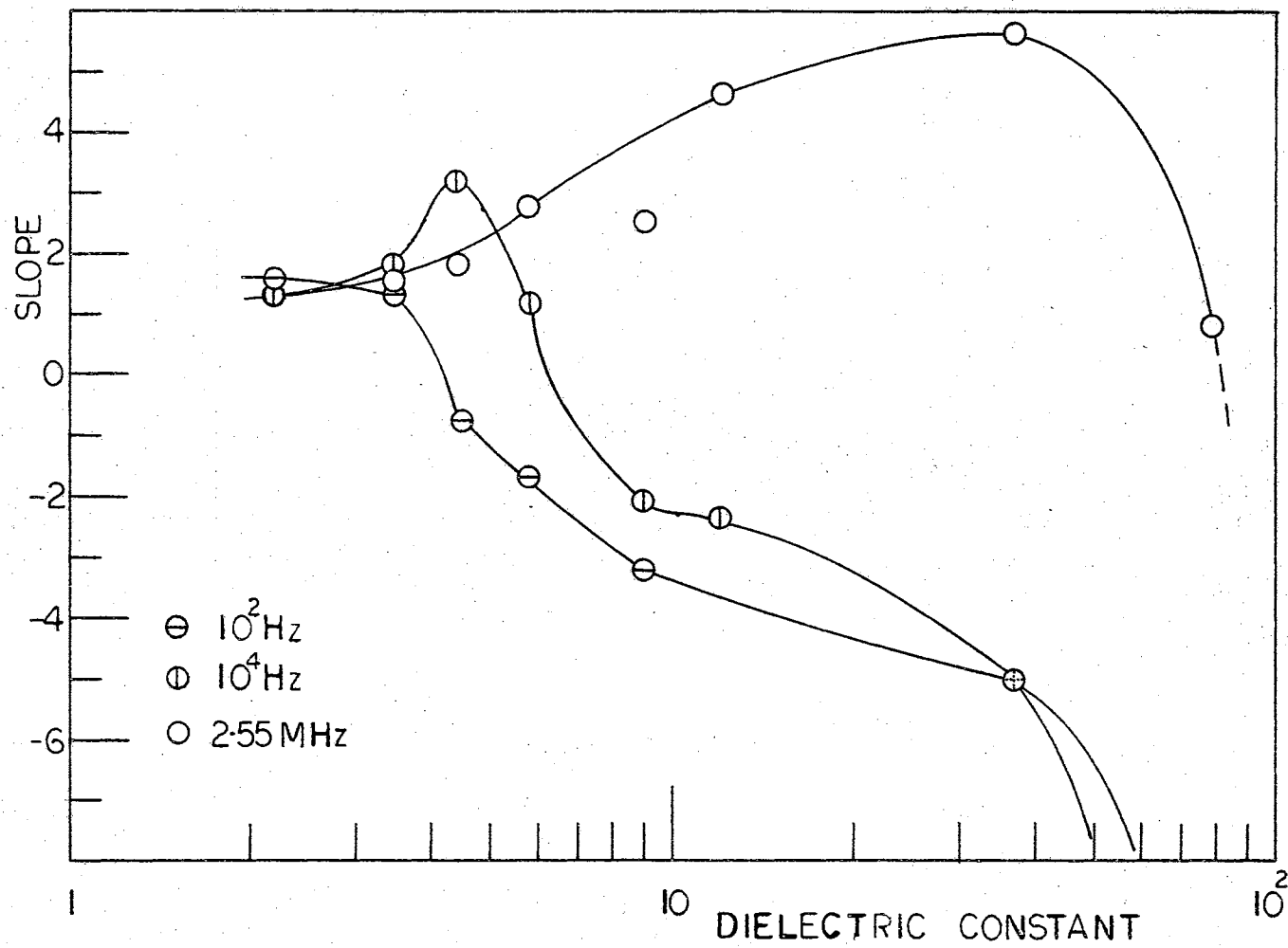


Figure 9. Slope Versus Dielectric Constant of Liquid for Rutile

The first set of graphs show the effect of the voltage on the dielectrophoretic force on the particle, this force being directly proportional to Z_{obs} .

The graphs in set one generally can be divided at the value 10, of the dielectric constant of the liquid medium, into two major ranges. The region with high resistivity of the liquid medium corresponds to the region with dielectric constant values 2.2 to 10, while low resistivity of the liquid medium corresponds to the region with dielectric constant values 10 - 80 of the liquid medium. Generally, in the region mentioned in the first instance above, the magnitude and direction of the force is independent of the frequency. In the other region the force is seen to differ for different frequencies.

The graphs show that different particles behave in characteristically different ways, i.e., the Z_{obs} (as defined on the previous page) is a function of frequency.

Silicon is deflected at all frequencies and in both regions in the positive direction, that is towards the electrode or region of highest field intensity. No cross-over point is exhibited.

The quartz particle was found to cross over at about 4.4 for all three frequencies used, i.e., at $K_2 = 4.4$. In the second region all the deflections are negative and the lowest frequency produces the greatest force. In the first region it is noted that all the forces after 4.4 are negative.

The responses of the tin particle in the first region are the same as each other at all three frequencies, but in the second region the higher frequency produces a greater deflection in the positive direction

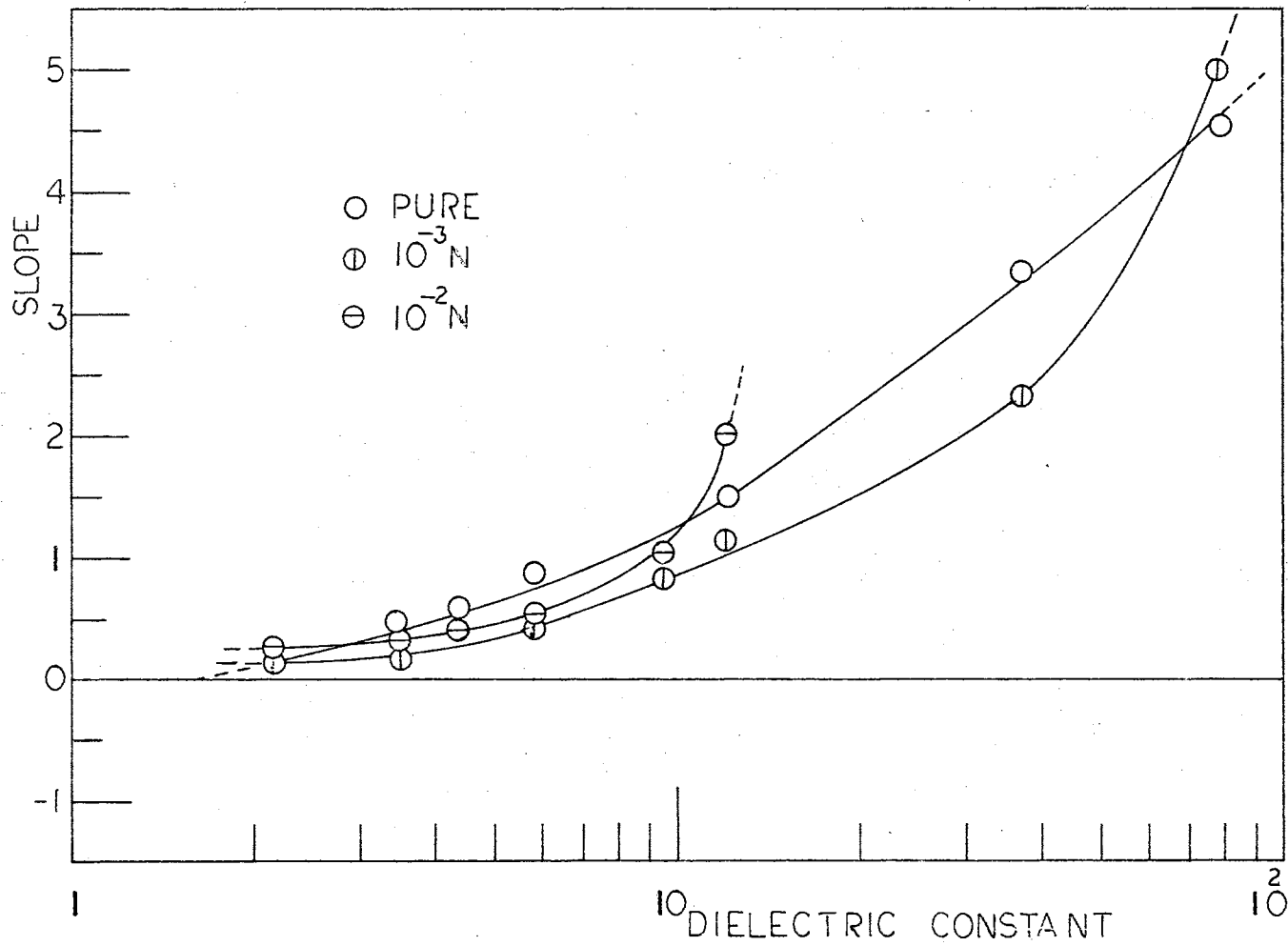


Figure 10. Slope Versus Dielectric Constant of Liquid for Silicon

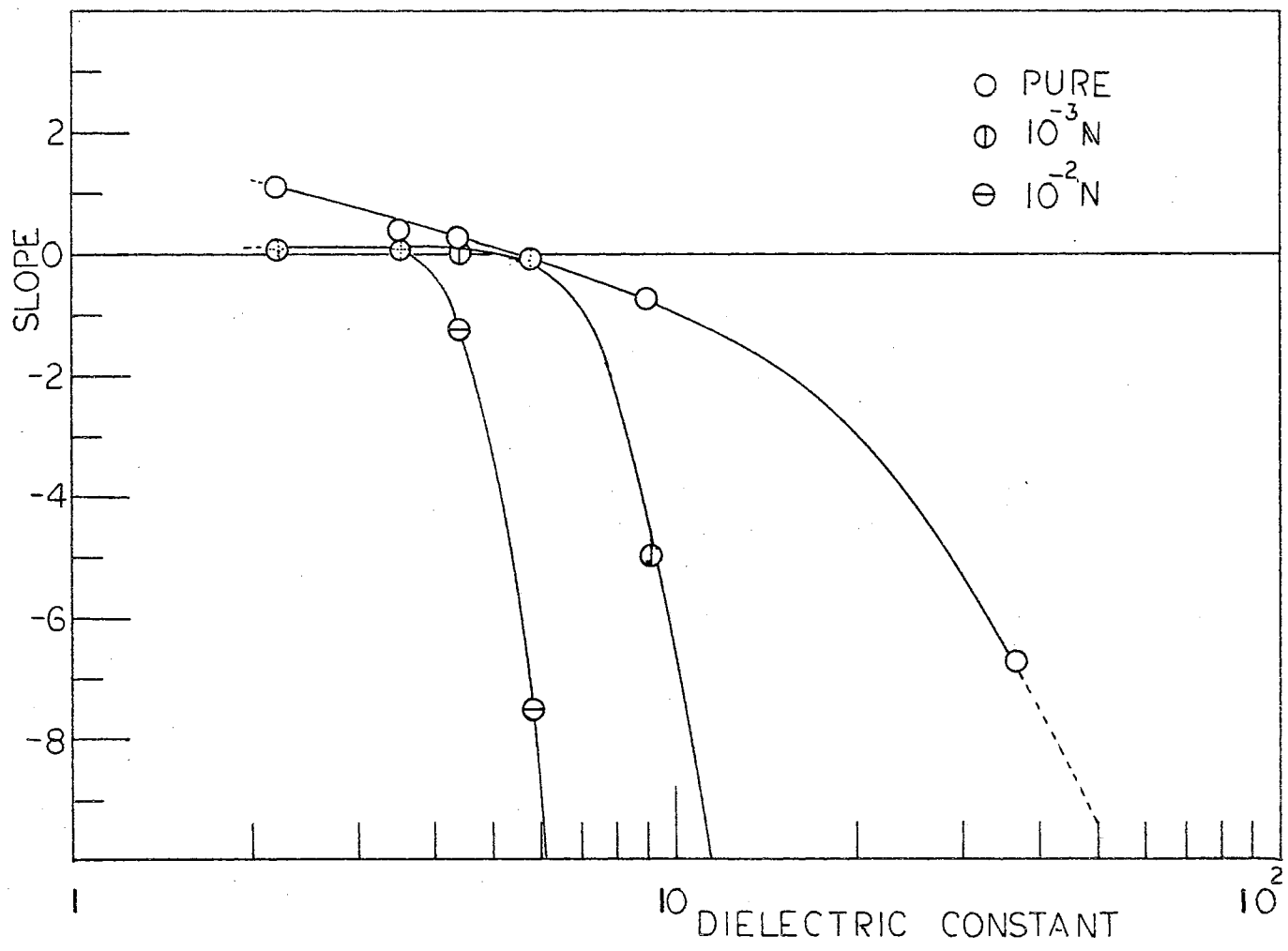


Figure 11. Slope Versus Dielectric Constant of Liquid for Silicon Dioxide

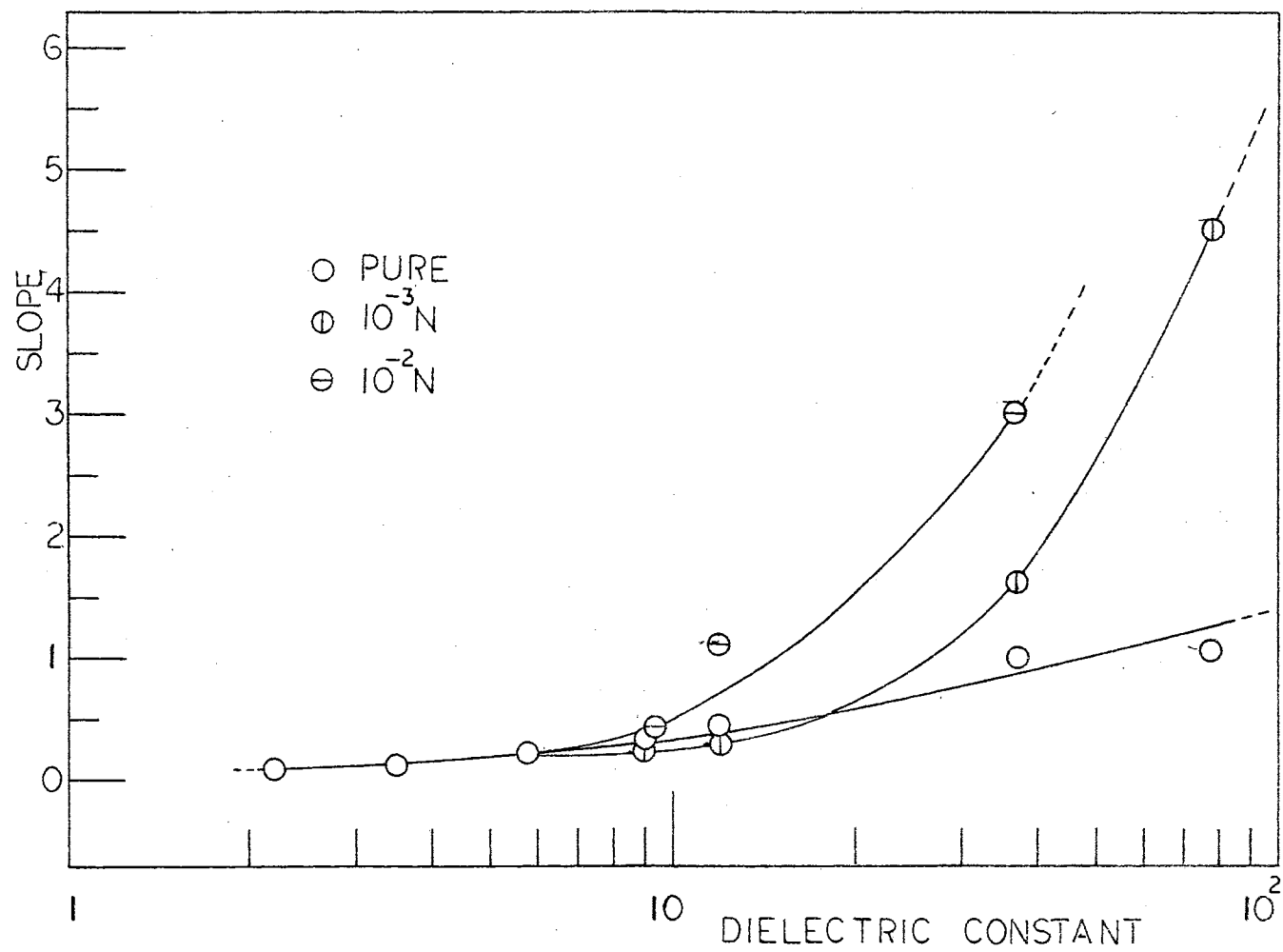


Figure 12. Slope Versus Dielectric Constant of Liquid for Tin

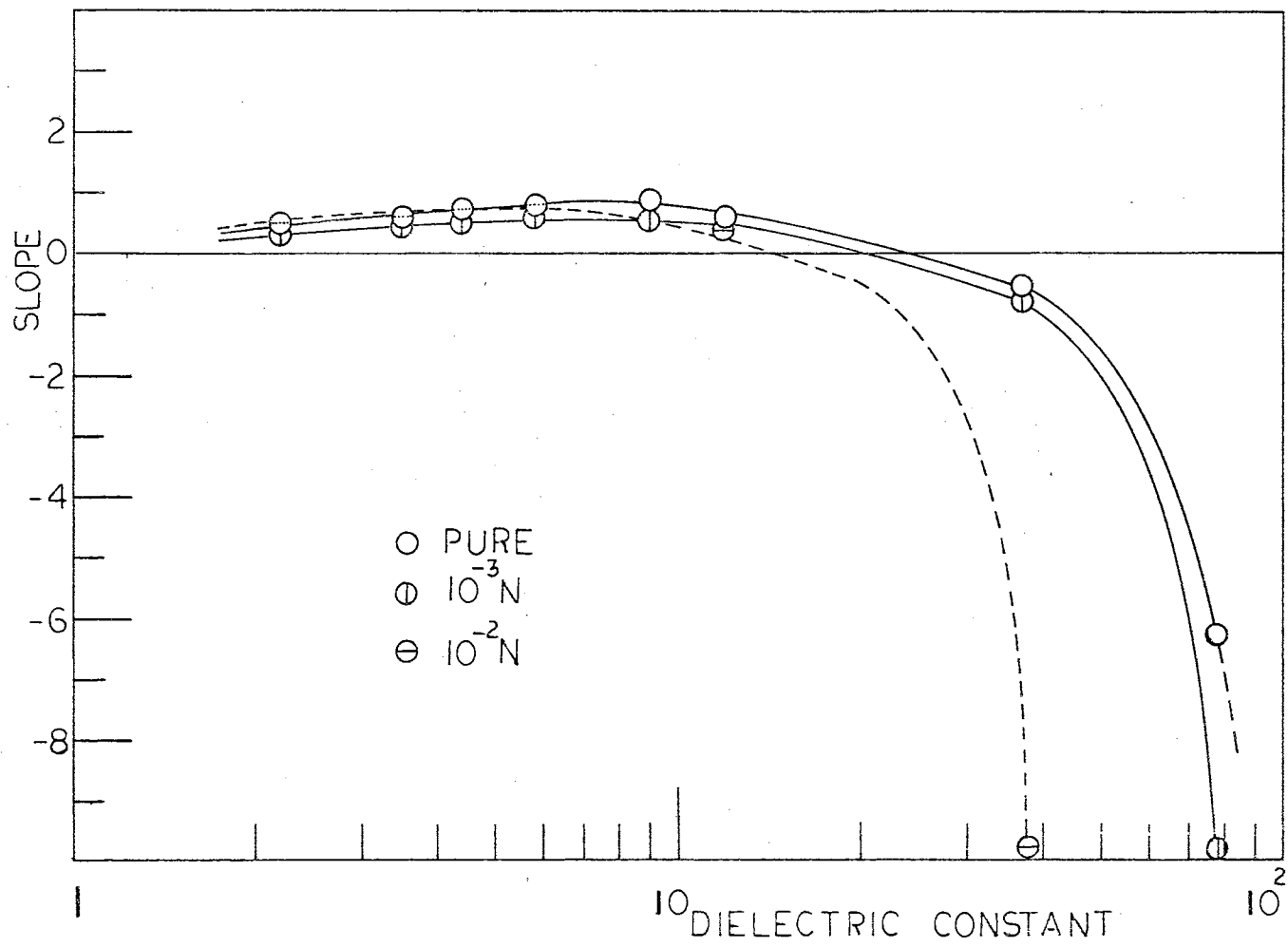


Figure 13. Slope Versus Dielectric Constant of Liquid for Stannic Oxide

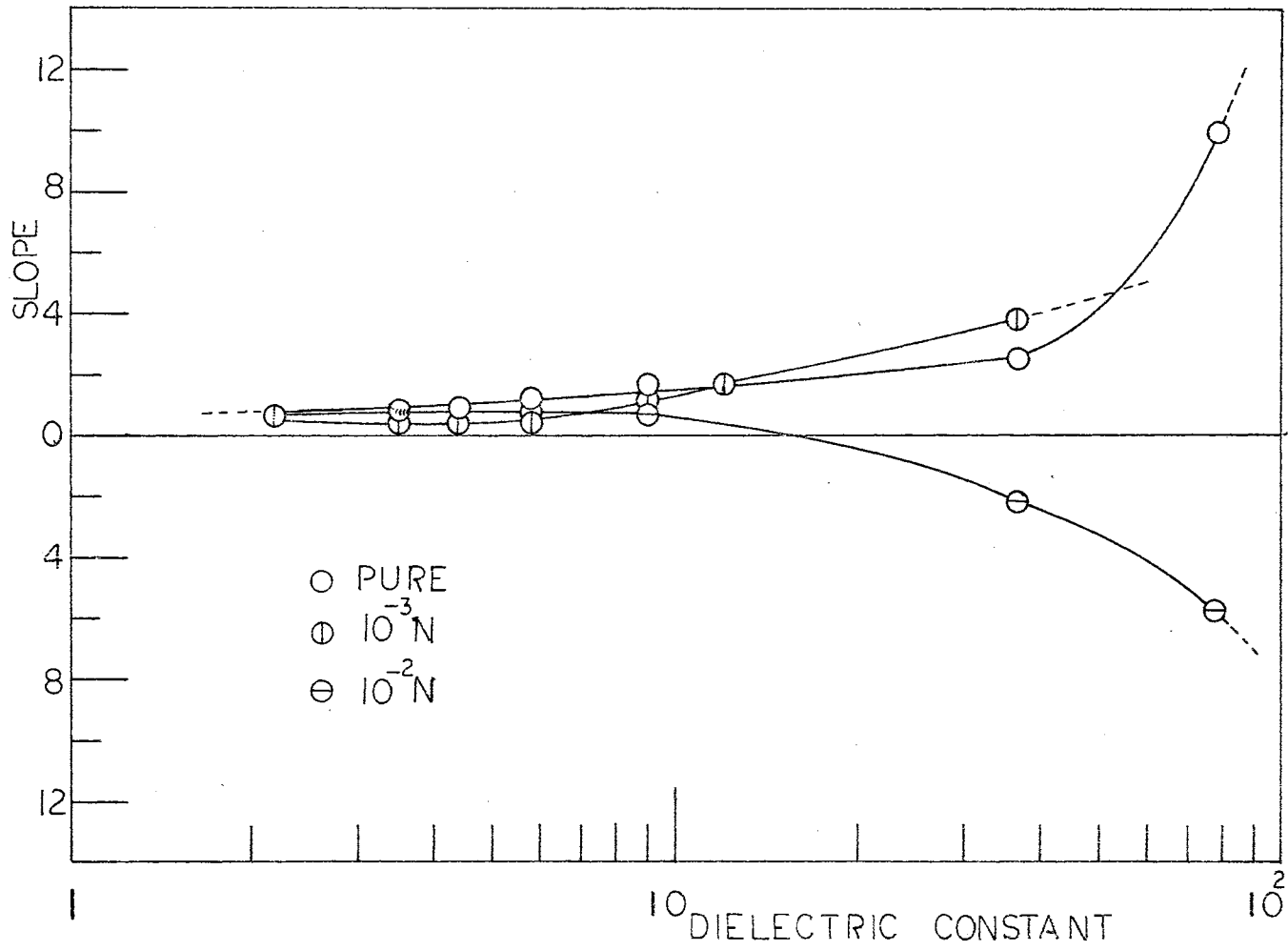


Figure 14. Slope Versus Dielectric Constant of Liquid for Lead Hafnate

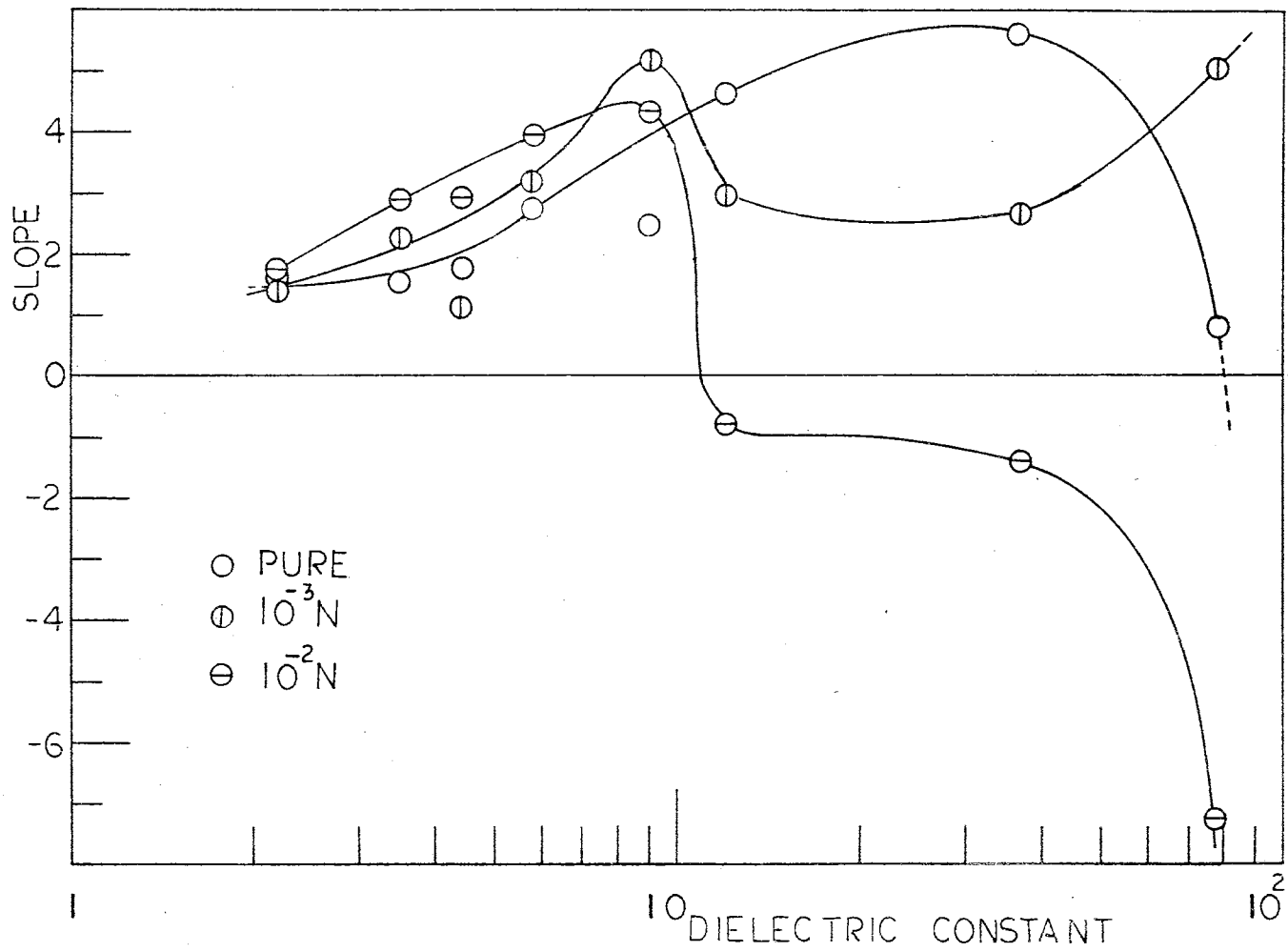


Figure 15. Slope Versus Dielectric Constant of Liquid for Rutile

than the two other frequencies.

The stannic oxide particle behaves in a similar manner to the quartz. The cross-over value for 2.55 MHz is at $K_2 = 27$. The other frequencies produce a cross-over of the particle in the first region.

The force differs greatly for different frequencies in region one for lead hafnate. The high frequency curve shows no cross-over.

Finally, the dielectrophoretic response of the rutile particles was found to be erratic, being particularly so at the lower frequencies, and the high frequency force appears to tend towards a cross-over beyond the second region.

The second set of graphs show the change in the force on the addition of the salt tetra-iso-pentylammonium nitrate to the liquid medium.

For silicon the addition of the salt produces an effect similar to the lowering of the frequency of the applied voltage, i.e., the magnitude of the positive force is reduced on increasing the concentration of the salt. For the highest concentration of salt the force is greatly increased when the liquids dielectric constant is greater than 10.

In the case of quartz the addition of the salt causes an increase of the force in the negative direction. The cross-over point is displaced to a lower value of K_1 than is found in the pure case. This displacement is again proportional to the concentration of the salt.

Where tin is concerned the salt increases the force in the positive direction, the increase again depending on the concentration of the salt.

For the remaining three particles, stannic oxide, lead hafnate and rutile, the behavior previously noted is similarly observed, i.e., a reduction of the dielectrophoretic force, and a displacement of cross-

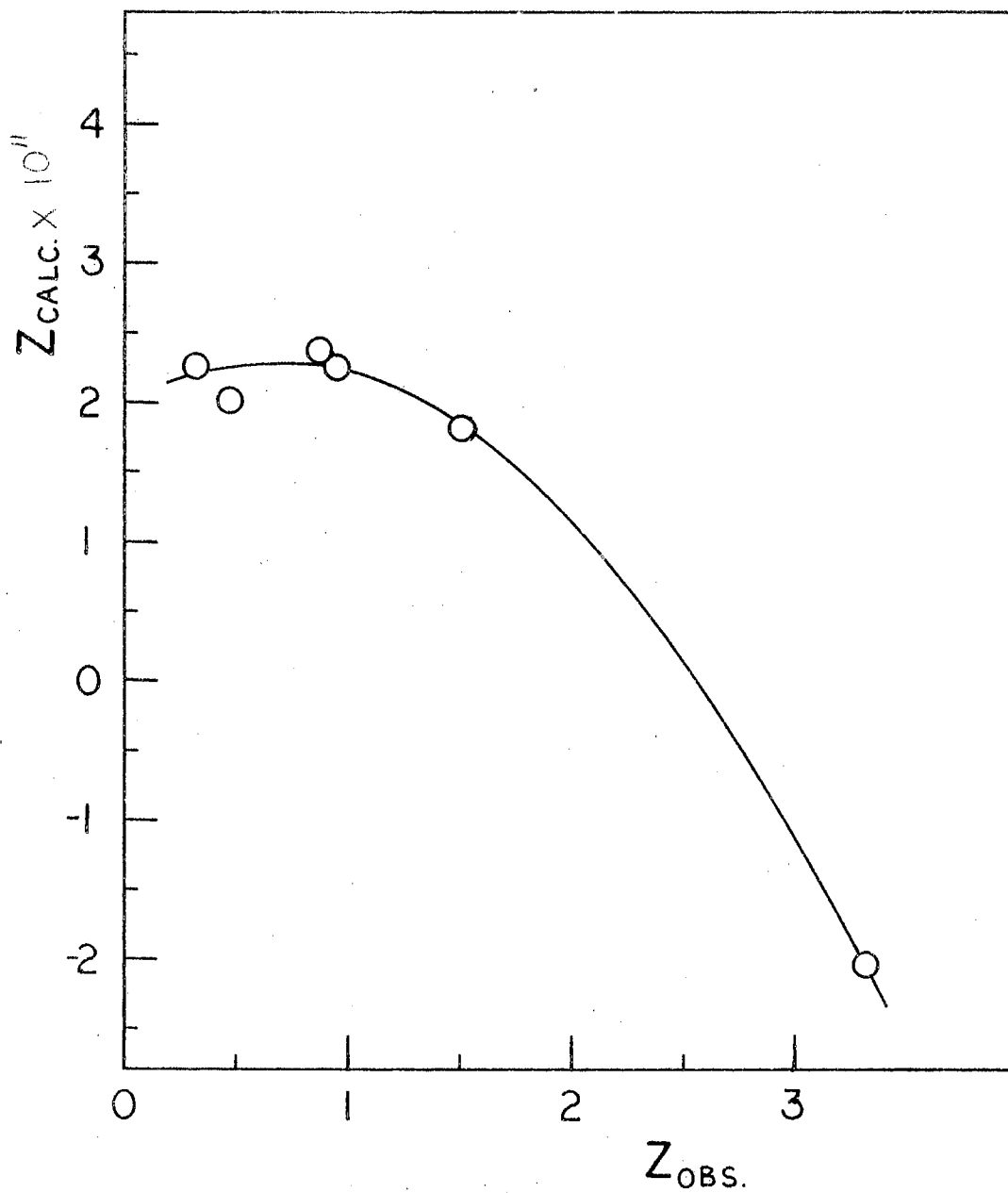


Figure 16. Calculated Slope Z_{calc} Versus Observed Slope Z_{obs} for Silicon

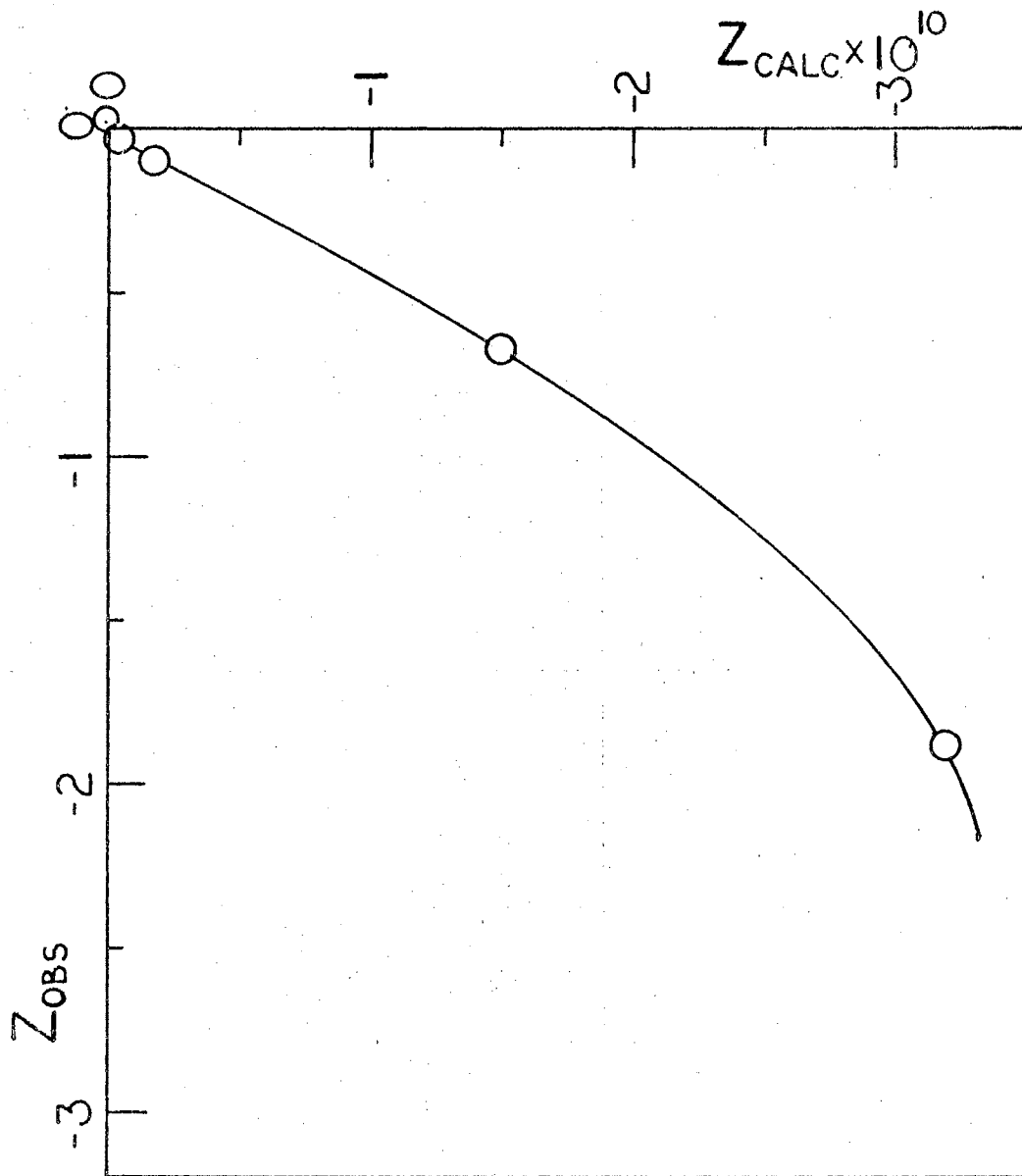


Figure 17. Calculated Slope Z_{calc} Versus Observed Slope Z_{obs} for Silicon Dioxide

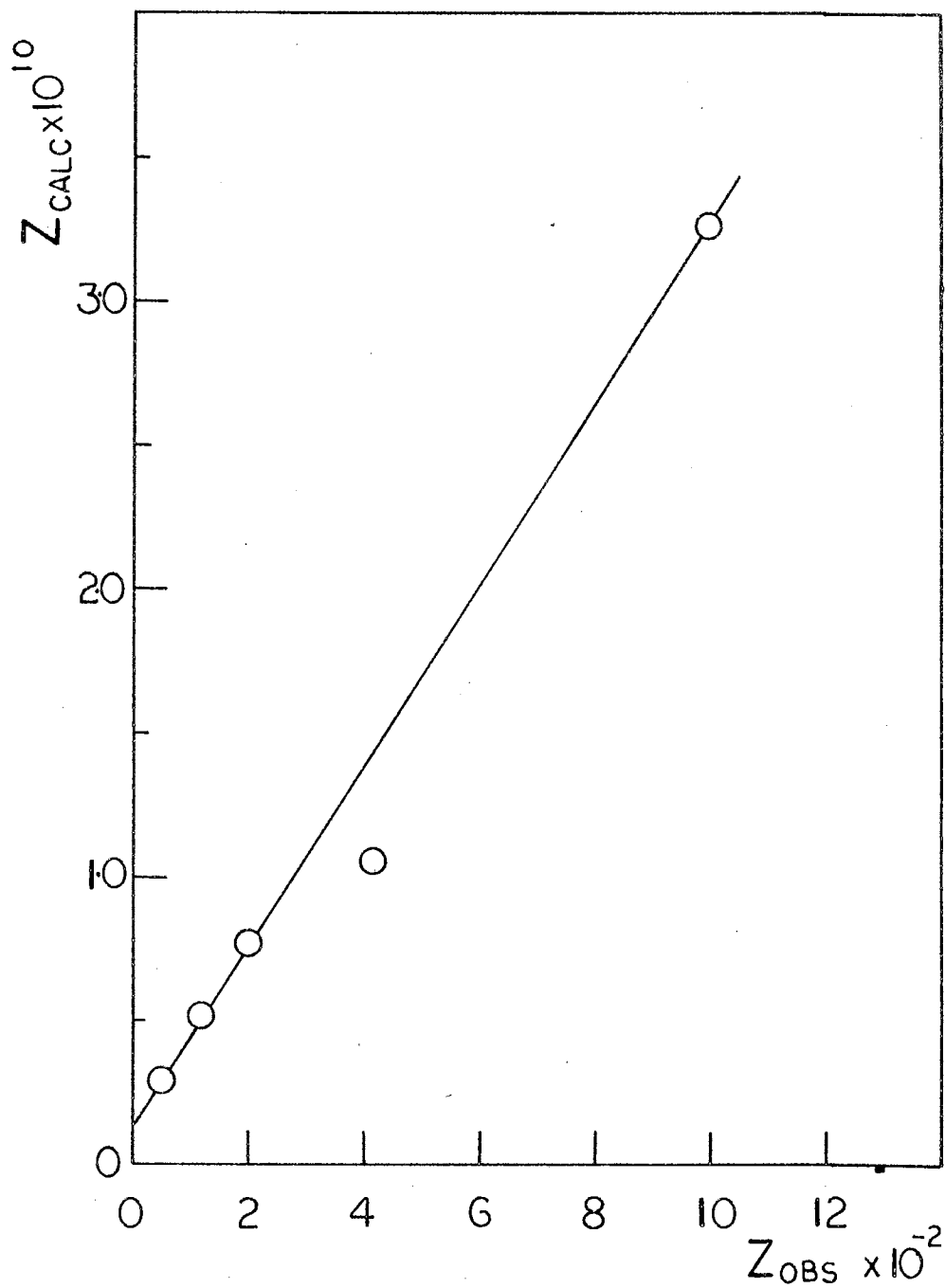


Figure 18. Calculated Slope Z_{calc} Versus Observed Slope Z_{obs} for Tin

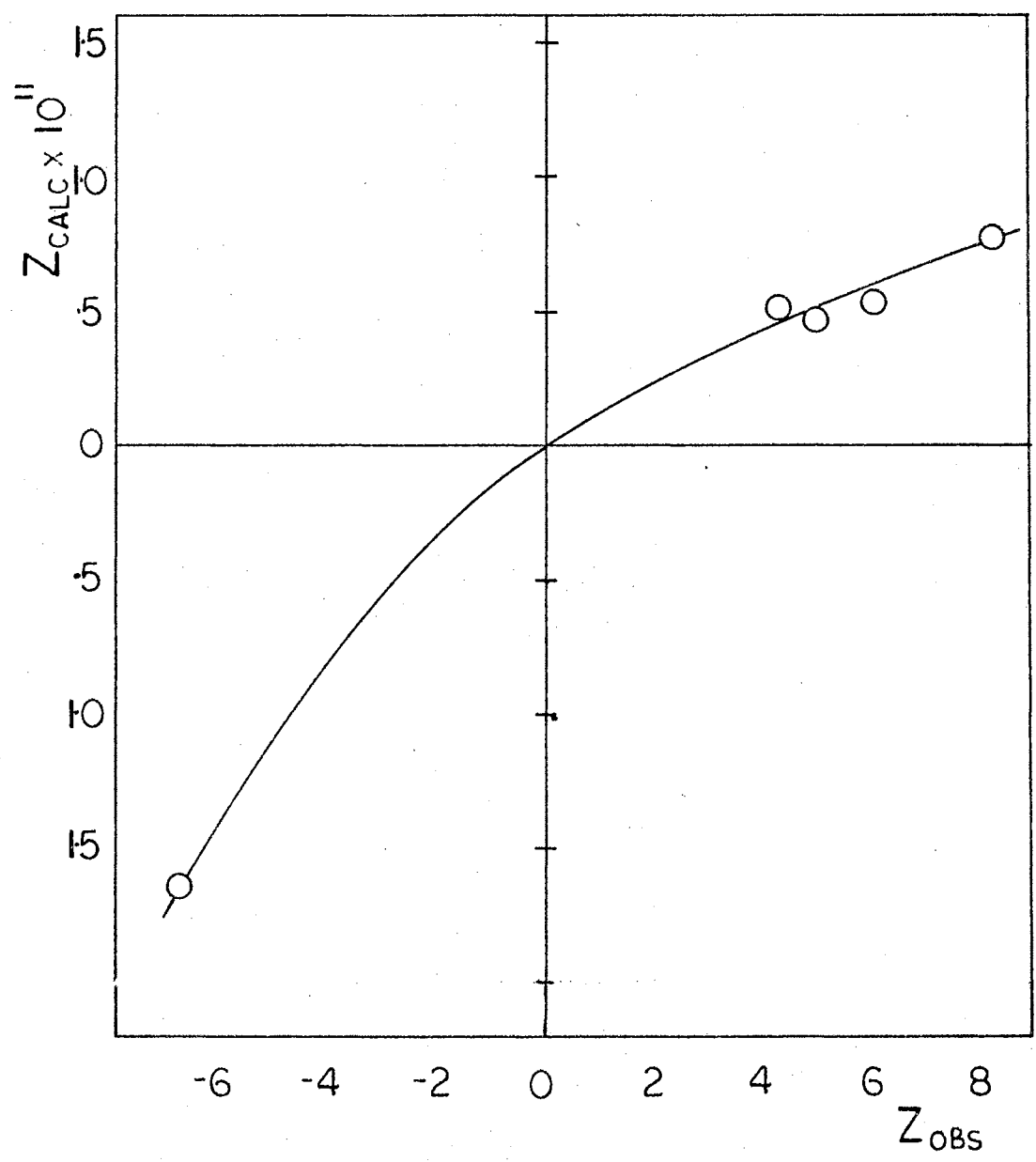


Figure 19. Calculated Slope Z_{calc} Versus Observed Slope Z_{obs} for Stannic Oxide

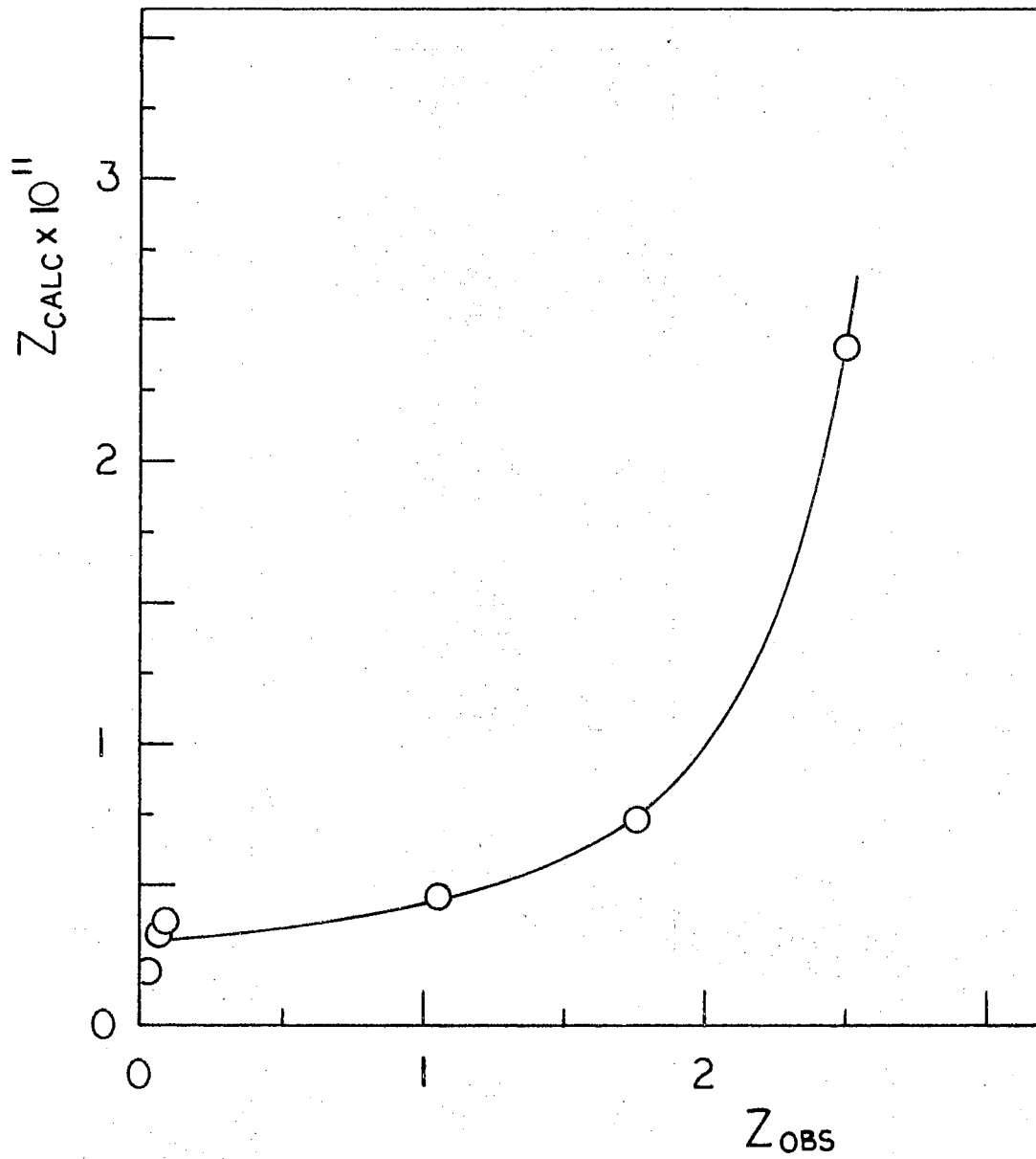


Figure 20. Calculated Slope Z_{calc} Versus Observed Slope Z_{obs} for Lead Hafnate

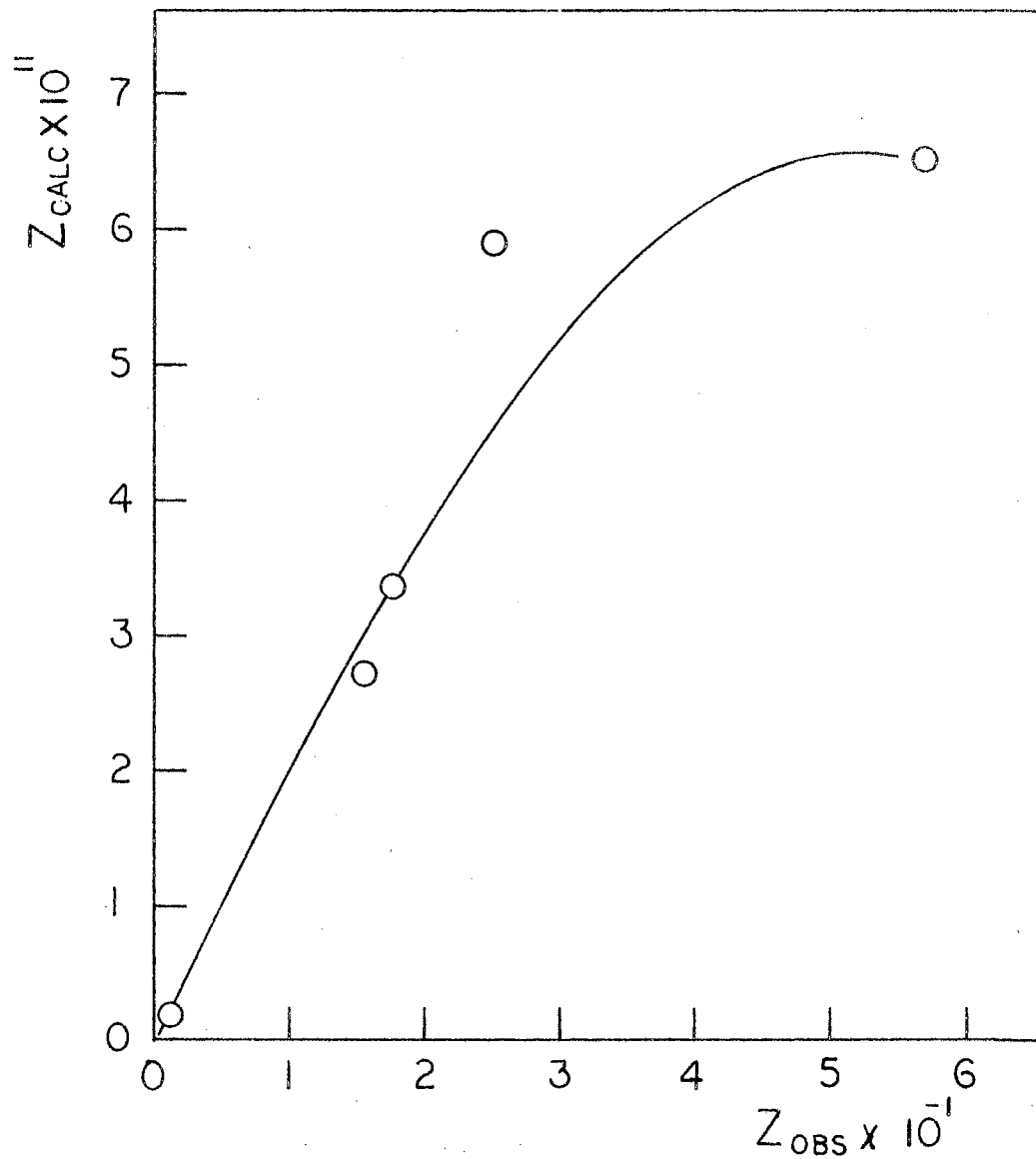


Figure 21. Calculated Slope Z_{calc} Versus Observed Slope Z_{obs} for Rutile

over points to values usually obtained using low frequencies.

In the third set of graphs the experimentally determined initial slope (i.e., $Z_{obs.}$) is plotted against the calculated theoretical initial slope. High frequency (2.55 MHz) voltage was used to eliminate the effects of electrode polarization, and the equation was tested using the dielectric constant and resistivity values of the particles and liquid media shown in the computer print-out.

The test of correlation between the theoretical force and the experimental one (I-2) is that when plotted they should exhibit common zeros and linearity.

The graphs for silicon and lead hafnate do not show correlation, the silicon being the most divergent from the theory. The graphs for the remaining particles show a tendency towards linearity and common zeros.

CHAPTER V

SUMMARY AND CONCLUSIONS

Brief Summary of the Work

The dielectrophoretic response of real particles of different materials, in liquid dielectrics differing in resistivity and dielectric constant, has been studied. The effect of the addition of the salt tetra-iso-pentylammonium nitrate to the liquid medium was also observed. The experimentally observed force was compared with that predicted by a theory which allowed for the conductivity of the materials.

Conclusions

For all the particles studied (except tin) an interesting general effect was observed: in the case of the pure liquid the addition of the salt to the liquid media reduced the dielectrophoretic force resulting from the high frequency voltage in the same manner as the force would be reduced if the frequency were lowered. As a result it appears that dielectrophoretic properties of particles should be measured at high frequencies.

For the silicon particle there is no correlation between the observed dielectrophoretic behavior and the theoretically calculated dielectrophoretic behavior. This may be due to not knowing the correct value of the dielectric constant of silicon, the value used being 12. This value for silicon was determined at a very high frequency 12 GHz,

(Table I). Recently it has been shown that there is a possibility of silicon having an extremely high dielectric constant, even at 2.55 MHz, the frequency used in this experiment¹⁸. The alternative explanation to an increase in the dielectric constant would be a drastic reduction in the resistivity of the silicon to 10^{-3} ohms-meter, which would then give the observed effects. The latter is most improbable.

The commonly accepted dielectric constant for silicon is twelve (see Table II) but its present experimental behavior indicates a far greater value if it is in an ionically conductive medium of high dielectric constant (see Figure 10). The increased effective dielectric constant may be due to the interaction of the current flowing in the liquid medium with ions adsorbed on the surface of the silicon (ionic double layer effect).

Energy states having energies distributed in the forbidden region between the valence and the conduction bands also exist at the surface of a semi-conductor. These surface states will be affected by surface charges due to adsorbed negative ions. (It is usual to see hydroxyl ions preferentially adsorbed on solids in contact with water¹⁹.) Electrical double layers will be built up, one on the liquid side and one on the solid side of the interface. At equilibrium the Fermi level of the surface states and that of the bulk material will tend to equalize. A surface layer within the crystal will form as electrons in the conduction band are repelled by the negative surface state charges and a net positive charge will exist in the resulting space charge region. As a result the energy bands are bent upwards, as illustrated.

The usual ionic Helmholtz double layer is caused by the preferential adsorption of negative ions from the liquid medium. Those adsorbed

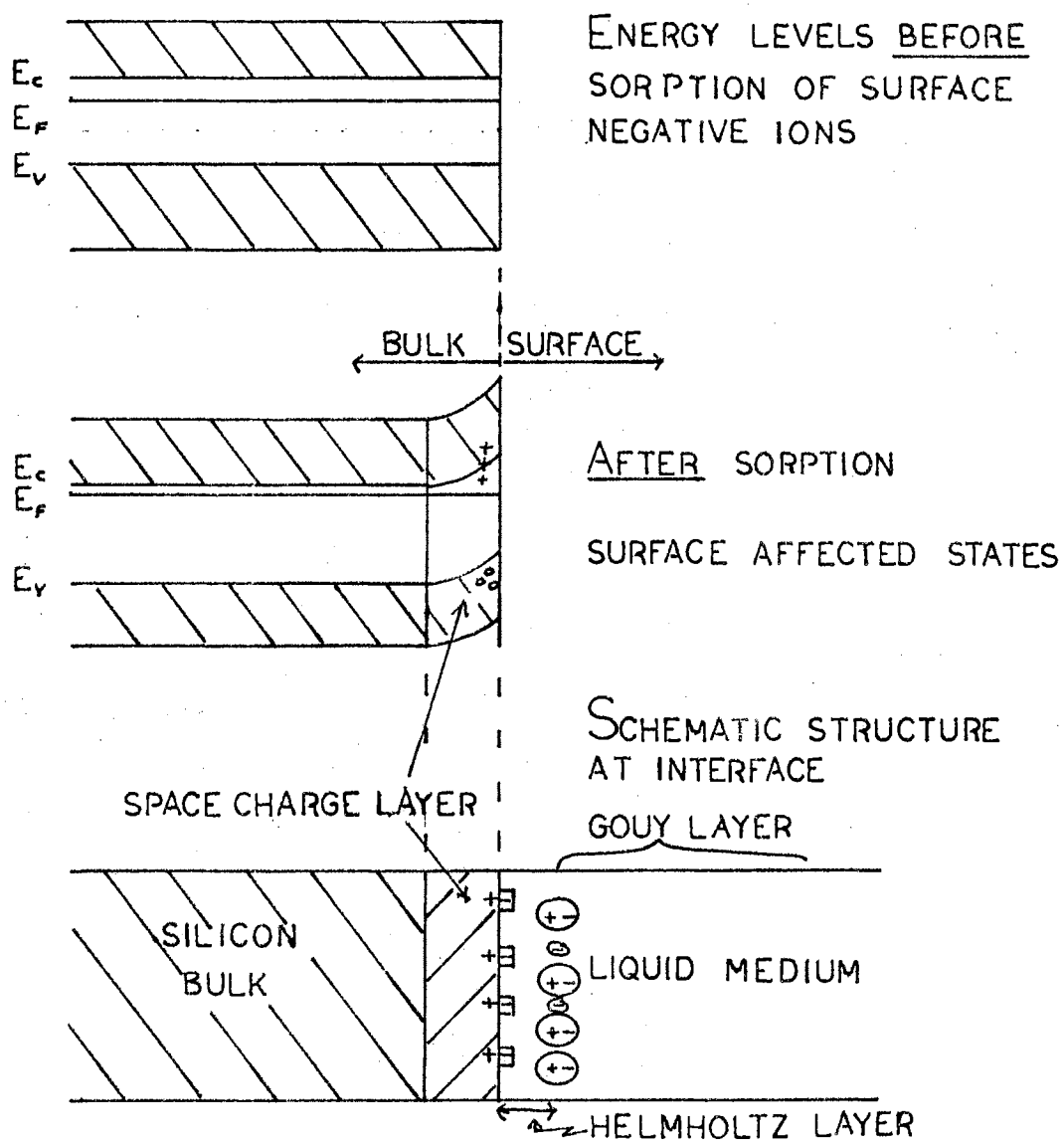


Figure 22. Schematic Structure, and Energy Levels Before and After Sorption of Surface Negative Ions

negative ions, on the side of the silicon facing the positive electrode will tend to be neutralized as current flows. This is caused by the positive ions in the current flowing toward the surface. Simultaneously the adsorbed negative ions on the far side of the particle should have their density increased. The net result will be an external dipole which acts externally as an increase in the effective dielectric constant of the particle.

The Enhancement of Bulk Liquid Polarization by Ions

Using the pure mixture curve as a reference line (see Figure 10) we note that two opposing effects are operating. As the dielectric constant of the liquid medium increases the addition of salt at first causes the silicon to be less attracted into the region of highest field strength. This, we believe, is a reflection of the increased polarization of the now conductive medium.

The Enhancement of Polarization of Solids by Ionic Double Layer

As the dielectric constant of the medium increases still further, however, the double layer effect can now be supported. This produces in turn a huge internal polarization in the semiconductor and in crystals which have large internal populations of free charge. The solid, because of its now higher effective polarization, acts, as it were, more polar than the liquid medium. We see this for silicon in the upturn and cross over of the slope against dielectric constant lines of the salt-added curves in Figure 2B.

Finally, there is no striking correlation between the theoretically calculated and the experimentally determined behavior for the rest of

the particles. For each, the best correlation is obtained for the highest resistivities of the liquid media.

BIBLIOGRAPHY

1. Gilbert, W. De Magnete, Book II, (Peter Short, London, 1600).
2. Winckler, F. H. Essai sur la Nature; Effects et les Causes de l'Electricite, Vol. I, (Sebastian Jorry, Paris, 1748).
3. Priestley, J. The History and Present State of Electricity with Original Experiments, (2nd ed.), (London, 1748).
4. Gyemant, A., *Wiss Veroff*, *Siem. Kons.* 5, No. 2, 55 (1926).
5. Greinacher, H. *Helv. Phys. Acta* 21, 261 (1948).
6. Hatscher, E. and P. C. L. Thorne, *Kolloid-Z.* 33, 1 (1923).
7. Soyenoff, B. C. *J. Phys. Chem.* 35, 2993 (1931).
8. Pohl, H. A. *J. Appl. Phys.* 32, 1784 (1961).
9. Pickard, W. F. *Progress in Dielectrics* 6, 105 (1965).
10. Pohl, H. A. *J. Electrochemical Society* 107, 386 (1960).
11. Hawk, I. L. Effects of non-uniform electric fields on real dielectrics in water. Master's Thesis, Oklahoma State University, 1967.
12. Abraham, M. and R. Becker. *Classical Theory of Electricity and Magnetism*, (2nd ed.), (Blackie and Son Ltd., 1950).
13. Sher, L. D. *Nature* 220, 695 (1968).
14. Stratton, J. A. *Electromagnetic Theory* (McGraw-Hill, New York, 1941), p. 136.
15. Kraus, C. A. and R. M. Fuoss. *Am. J. of Chem.* 55, 21 (1933).
16. Hasted, J. B. and D. M. Ritson and C. H. Collie. *F. Chem. Phys.* 16, 1 (1948).
17. Baum, G. Dispersion of the dielectric characteristics in lead zirconate stannate titanate and lead hafnate exhibiting ferroelectricity and/or antiferroelectricity. Master's Thesis, Oklahoma State University, 1964.
18. Iglesias, J. and W. B. Westphal. *Tech. Rep. 203*, Lab. Ins. Res.

MIT, 1967.

19. Glasstone, S. Physical Chemistry, p. 1227 (2nd ed., D. Van Nostrand Co., Inc. 1946).
20. Schwarz, G. J. Chem. Phys. 39, 2387 (1963).

APPENDIX

COMPUTING PROGRAM

```

$JOB 2233-50007 C. M. FEELEY
C INITIAL SLOPE OF THE FORCE EQN. COMPLEX C. M. FEELEY
1 COMPLEX E1,E2,CMLPX,CONJG
2 REAL K1,K2
3 WRITE(6,10)
4 10 FORMAT(1H1,2X,2HK1,7X,2HK2,5X,5HF(KC),5X,2HP1,9X,2HP2,11X,
12HZ1,12X,2HZ2,12X,5HZOBS,11X, 13X)
5 PI=3.1415927
6 EO=8.854E-12
7 1 READ(5,20)K1,K2,F,P1,P2,ZOBS
8 20 FORMAT(F6.0,2E12.4,4P2E12.4,0PF9.0)
9 EQW=2.0*PI*F
10 S1=1.0/EQW/P1
11 S2=1.0/EQW/P2
12 EP1=EO*K1
13 EP2=EO*K2
14 E1=CMLPX(EP1,-S1)
15 E2=CMLPX(EP2,-S2)
16 Z1=REAL(CONJG(E1)*(E2-E1)/(E2+2.*E1))
17 Z2=REAL((E1)*(E2-E1)/(E2+2.*E1))
18 IFKC=F/1000.0
19 WRITE (6,30) K1,K2,IFKC,P1,P2,ZOBS,Z1,Z2
20 30 FORMAT(1H0,F5.1,F9.1,I8,(1P)E11.1,E11.1,E14.4,F14.4,E15.4,
1E15.4)
21 GO TO 1
22 END

```

\$ENTRY

K1	K2	F(KC)	P1	P2	Z OBS	Z1	Z2
4.4	24.0	10	1.8E 05	1.1E-06	1.1400E 02	3.8958E-11	3.8958E-11
3.5	24.0	10	3.0E 05	1.1E-06	1.6100E 02	3.0989E-11	3.0989E-11
2.2	24.0	10	1.0E 06	1.1E-06	5.9000E 01	1.9479E-11	1.9479E-11
78.0	24.0	0	6.5E 02	1.1E-06	3.2300E 02	6.9061E-10	6.9061E-10
37.0	24.0	0	4.8E 02	1.1E-06	7.5000E 02	3.2760E-10	3.2760E-10
12.0	24.0	0	7.8E 03	1.1E-06	2.8600E 02	1.0625E-10	1.0625E-10
9.0	24.0	0	1.5E 04	1.1E-06	7.0000E 02	7.9686E-11	7.9686E-11
5.8	24.0	0	5.0E 04	1.1E-06	2.2900E 02	5.1353E-11	5.1353E-11
4.4	24.0	0	1.8E 05	1.1E-06	1.1900E 02	3.8958E-11	3.8958E-11
3.5	24.0	0	3.0E 05	1.1E-06	7.5000E 02	3.0989E-11	3.0989E-11
2.2	24.0	0	1.0E 06	1.1E-06	5.9000E 01	1.9479E-11	1.9479E-11
78.0	86.0	0	1.0E 02	1.0E 13	-1.9200E 02	-9.1639E-10	2.2579E-10
37.0	86.0	0	4.2E 02	1.0E 13	-5.0000E 01	-7.3488E-10	4.0728E-10
12.0	86.0	0	6.2E 03	1.0E 13	-8.1000E 00	-6.2420E-10	5.1796E-10
5.8	86.0	0	1.5E 04	1.0E 13	-1.6600E 01	-5.9675E-10	5.4540E-10
4.4	86.0	0	2.0E 05	1.0E 13	-8.3000E 00	-5.8883E-10	5.5017E-10
3.5	86.0	0	2.5E 05	1.0E 13	1.2700E 01	-5.8402E-10	5.5339E-10
2.2	86.0	0	1.0E 06	1.0E 13	1.5400E 01	-5.4521E-10	5.2903E-10
78.0	86.0	10	1.0E 03	1.0E 13	-2.5000E 02	-9.1215E-10	2.2486E-10
12.0	86.0	10	6.2E 03	1.0E 13	-2.3100E 01	-6.0004E-10	5.0245E-10
5.8	86.0	10	1.5E 04	1.0E 13	1.2500E 01	-5.0587E-10	4.7383E-10
4.4	86.0	10	2.0E 05	1.0E 13	3.2100E 01	1.1873E-11	5.1613E-11
3.5	86.0	10	2.5E 05	1.0E 13	1.7500E 01	1.3151E-11	3.9822E-11
2.2	86.0	10	1.0E 06	1.0E 13	1.1400E 01	1.7111E-11	1.8915E-11
37.0	86.0	2550	4.2E 02	1.0E 13	5.7300E 01	6.5115E-11	1.1327E-10
12.0	86.0	2550	6.2E 03	1.0E 13	4.7200E 01	7.1179E-11	7.1667E-11
9.0	86.0	2550	1.0E 04	1.0E 13	2.5000E 01	5.8975E-11	5.9085E-11
4.4	86.0	2550	2.0E 05	1.0E 13	1.7500E 01	3.3533E-11	3.3533E-11
3.5	86.0	2550	2.5E 05	1.0E 13	1.5500E 01	2.7490E-11	2.7490E-11
78.0	24.0	10	4.6E 02	2.7E 05	-1.0900E 02	-5.0249E-10	-1.8622E-10
37.0	24.0	10	3.2E 02	2.7E 05	-2.5000E 01	-3.2238E-10	-4.6183E-12
78.0	24.0	2550	4.6E 02	2.7E 05	-1.0000E 02	-2.1552E-10	-2.0659E-10
37.0	24.0	2550	3.2E 02	2.7E 05	-6.7000E 00	-9.0402E-11	-3.6920E-11
9.0	24.0	0	9.0E 03	2.7E 05	-7.9000E-01	-1.9015E-10	1.1438E-10
9.0	24.0	10	9.0E 03	2.7E 05	-7.2000E 00	-1.8783E-10	1.1347E-10
12.0	24.0	10	4.7E 03	2.7E 05	-5.0000E 00	-2.0612E-10	1.0322E-10
12.0	24.0	0	4.7E 03	2.7E 05	-6.3000E 00	-2.0702E-10	1.0352E-10
78.0	11.9	2550	1.0E 02	5.0E 02	4.5400E 02	-2.5298E-10	-2.7168E-10
12.0	11.9	2550	3.3E 02	5.0E 02	3.3500E 02	-2.0469E-11	8.8789E-13
12.0	11.9	2550	5.2E 03	5.0E 02	1.5000E 02	1.7748E-11	1.0733E-11
9.0	11.9	2550	1.0E 04	5.0E 02	9.6300E 01	2.2635E-11	1.8724E-11
5.8	11.9	2550	2.8E 04	5.0E 02	8.7500E 01	2.3869E-11	2.2493E-11
4.4	11.9	2550	8.8E 04	5.0E 02	3.3400E 01	2.2104E-11	2.1692E-11
2.2	11.9	2550	2.0E 05	5.0E 02	8.3000E 00	1.4885E-11	1.4882E-11
3.5	11.9	2550	1.0E 05	5.0E 02	4.6300E 01	2.0002E-11	1.9678E-11
37.0	11.9	10	3.3E 02	5.0E 02	2.5000E 02	5.1235E-12	-8.8874E-11
12.0	11.9	10	5.2E 03	5.0E 02	1.3400E 02	1.0004E-10	6.1035E-11
9.0	11.9	10	1.0E 03	5.0E 02	1.3090E 02	3.0048E-11	9.7947E-12
9.0	11.9	10	1.0E 04	5.0E 02	1.0710E 02	7.8041E-11	5.9591E-11
5.8	11.9	10	2.8E 04	5.0E 02	8.3300E 01	5.1166E-11	4.6225E-11
4.4	11.9	10	2.8E 04	5.0E 02	8.3300E 01	3.8793E-11	3.5090E-11
3.5	11.9	10	1.0E 05	5.0E 02	5.3000E 01	3.0976E-11	3.0080E-11
2.2	11.9	10	2.0E 05	5.0E 02	8.7000E 00	1.9476E-11	1.9191E-11
78.0	11.9	0	1.0E 02	5.0E 02	2.3800E 02	-2.3083E-10	-2.7144E-10
37.0	11.9	0	3.3E 02	5.0E 02	1.8700E 02	5.1270E-12	-8.8874E-11
12.0	11.9	0	5.2E 03	5.0E 02	1.2500E 02	1.0005E-10	6.1039E-11
9.0	11.9	0	1.0E 04	5.0E 02	1.2500E 02	7.8045E-11	5.9594E-11
5.8	11.9	0	2.8E 04	5.0E 02	7.6900E 01	5.1168E-11	4.5226E-11
4.4	11.9	0	8.8E 04	5.0E 02	8.3000E 00	3.8940E-11	3.7662E-11
3.5	11.9	0	1.0E 05	5.0E 02	5.0000E 01	3.0977E-11	3.0081E-11
2.2	11.9	0	2.0E 05	5.0E 02	7.3000E 00	1.9476E-11	1.9191E-11

K1	K2	F(KC)	P1	P2	ZObs	Z1	Z2
12.0	24.0	2550	4.7E 03	2.7E 05	6.3000E 00	2.5637E-11	2.6887E-11
9.0	24.0	2550	9.0E 03	2.7E 05	8.3000E 00	2.9145E-11	2.9593E-11
5.8	24.0	2550	3.0E 04	2.7E 05	4.3000E 00	2.6217E-11	2.6271E-11
4.4	24.0	2550	9.6E 04	2.7E 05	5.0000E 00	2.3276E-11	2.3292E-11
3.5	24.0	2550	1.8E 05	2.7E 05	5.0000E 00	2.0492E-11	2.0493E-11
5.8	24.0	0	3.0E 04	2.7E 06	-7.3000E 00	-1.8244E-10	1.3194E-10
3.5	24.0	0	1.8E 05	2.7E 05	5.4000E 00	-3.4790E-11	7.7050E-11
2.2	24.0	0	1.0E 06	2.7E 05	6.3000E 00	-3.6950E-12	2.2171E-11
5.8	24.0	10	3.0E 04	2.7E 05	5.3000E 00	-1.4709E-10	1.1097E-10
4.4	24.0	10	9.6E 04	2.7E 05	4.4000E 00	-6.7730E-11	7.0533E-11
3.5	24.0	10	1.8E 05	2.7E 05	5.8000E 00	-2.4218E-11	4.4511E-11
2.2	24.0	10	1.0E 06	2.7E 05	5.0000E 00	1.2800E-11	1.5785E-11
78.0	3.7	2550	4.8E 02	1.0E 18	1.8600E 00	-3.2289E-10	-3.2129E-10
37.0	3.7	2550	3.3E 02	1.0E 18	6.7000E-01	-1.5153E-10	-1.4013E-10
12.0	3.7	2550	1.0E 03	1.0E 18	-3.0000E-01	-4.1271E-11	-3.1161E-11
9.0	3.7	2550	8.4E 03	1.0E 18	-7.7000E-02	-1.9730E-11	-1.9438E-11
5.8	3.7	2550	2.8E 04	1.0E 18	-4.0000E-03	-7.3952E-12	-7.0421E-12
4.4	3.7	2550	9.2E 04	1.0E 18	2.7000E-02	-2.1879E-12	-2.1805E-12
3.5	3.7	2550	2.8E 05	1.0E 18	3.9000E-02	5.7834E-13	5.7942E-13
2.2	3.7	2550	5.0E 06	1.0E 18	1.1600E-01	3.6072E-12	3.6072E-12
78.0	3.7	10	4.8E 02	1.0E 18	-2.5000E 02	-3.6985E-10	-3.2074E-10
37.0	3.7	10	1.8E 02	1.0E 14	0.0000E-01	-1.3837E-10	-1.3923E-10
12.0	3.7	10	1.0E 02	1.0E 18	-1.3500E 01	-7.7694E-11	-2.8554E-11
9.0	3.7	10	8.4E 03	1.0E 18	-2.5000E 01	-6.4298E-11	-1.5294E-11
9.0	3.7	10	1.1E 03	1.0E 14	-2.5000E 02	-6.4411E-11	-1.5273E-11
4.4	3.7	10	9.2E 04	1.0E 18	2.4000E 00	-4.0162E-11	4.4160E-12
3.5	3.7	10	2.8E 05	1.0E 18	3.9000E 00	-2.3407E-11	5.5932E-12
2.2	3.7	10	5.0E 05	1.0E 18	4.7000E 00	-1.3103E-11	8.5534E-12
37.0	3.7	0	3.3E 02	1.0E 18	0.0000E-01	-1.8837E-10	-1.3023E-10
37.0	350.0	2550	4.5E 03	1.0E 14	2.5000E-01	2.4169E-10	2.4194E-10
9.0	350.0	2550	1.2E 04	1.0E 14	1.7000E-01	7.3815E-11	7.3362E-11
5.8	350.0	2550	1.1E 04	1.0E 14	1.0000E-01	4.8852E-11	4.8910E-11
4.4	350.0	2550	2.7E 05	1.0E 14	8.0000E-02	3.7524E-11	3.7524E-11
3.5	350.0	2550	3.0E 05	1.0E 14	7.0000E-02	3.0077E-11	3.0078E-11
2.2	350.0	2500	3.0E 05	1.0E 14	2.0000E-02	1.9116E-11	1.9116E-11
78.0	350.0	10	1.0E 03	1.0E 14	-8.3000E-01	-2.6104E-09	-2.4194E-09
37.0	350.0	10	4.5E 03	1.0E 14	-2.4000E-01	-1.4881E-09	1.7397E-09
12.0	350.0	10	1.3E 03	1.0E 14	-2.0000E-02	-2.3362E-09	2.2349E-09
9.0	350.0	10	1.2E 04	1.0E 14	1.0000E-02	-8.9788E-10	9.5493E-10
4.4	350.0	10	2.7E 05	1.0E 14	2.0000E-02	3.4250E-11	4.0642E-11
3.5	350.0	10	3.9E 05	1.0E 14	6.0000E-02	2.8499E-11	3.1596E-11
2.2	350.0	10	1.0E 06	1.0E 14	2.0000E-02	1.8874E-11	1.9352E-11
78.0	350.0	0	1.0E 03	1.0E 14	-2.2600E 00	-2.6695E-09	1.9739E-09
9.0	350.0	0	1.2E 04	1.0E 14	0.0000E-01	-2.3637E-09	2.2840E-09
5.8	350.0	0	4.0E 04	1.0E 14	-6.0000E-02	-2.3460E-09	2.2949E-09
4.4	350.0	0	2.7E 05	1.0E 14	-5.0000E-02	-2.1825E-09	2.1512E-09
3.5	350.0	0	3.0E 05	1.0E 14	-8.0000E-02	-2.1465E-09	2.1229E-09
78.0	24.0	0	4.6E 02	2.7E 05	6.8200E 01	-5.0264E-10	-1.8620E-10
37.0	24.0	2550	4.8E 02	1.1E-06	1.0000E 03	3.2760E-10	3.2760E-10
12.0	24.0	2550	7.8E 03	1.1E-06	4.2800E 02	1.0625E-10	1.0625E-10
9.0	24.0	2550	1.4E 04	1.1E-06	2.0000E 02	7.9636E-11	7.9636E-11
5.8	24.0	2550	5.0E 04	1.1E-06	1.1300E 02	5.1353E-11	5.1353E-11
4.4	24.0	2550	1.8E 03	1.1E-06	1.1500E 02	3.8958E-11	3.8958E-11
3.5	24.0	2550	3.0E 05	1.1E-06	5.4000E 01	3.0989E-11	3.0989E-11
78.0	24.0	10	6.5E 02	1.1E-06	3.1300E 02	6.9061E-10	6.9061E-10
37.0	24.0	10	4.8E 02	1.1E-06	1.0000E 03	3.2760E-10	3.2760E-10
12.0	24.0	10	7.8E 04	1.1E-06	2.8600E 02	1.0625E-10	1.0625E-10
9.0	24.0	10	1.4E 04	1.1E-06	3.3300E 02	7.9686E-11	7.9686E-11
5.8	24.0	10	3.0E 04	1.1E-06	2.5800E 02	5.1353E-11	5.1353E-11

VITA 1

Cyprian Michael Feeley

Candidate for the Degree of

Master of Science

Thesis: DIELECTROPHORESIS OF SOLIDS IN LIQUIDS OF DIFFERING DIELECTRIC CONSTANT AND CONDUCTIVITY

Major Field: Physics

Biographical:

Personal Data: Born in Dublin City, Ireland, September 16, 1939, the son of Michael Joseph and Mary Catherine Feeley.

Education: Attended St. Paul's College, Sybil Hill, Raheny, Dublin, graduating in 1959; received the honor degree of B.A. in Natural Sciences (specializing in experimental physics) from the University of Dublin, Trinity College, in 1964; completed the requirements for the Master of Science degree in August, 1969.

Professional Experience: Held research appointment, performing individual research on the dielectric properties of thin polymer films formed in a glow discharge, with the Electrical Research Association, Leatherhead, Surrey, England, in 1965; held physics teaching appointment, teaching general physics and engineering physics, with The City of Dublin Vocational Education Committee in 1966-1967. Held Teaching Assistantship at Oklahoma State University, in Fall Semester, 1967. Has held Research Assistantship at Oklahoma State University since beginning of Spring Semester, 1968.